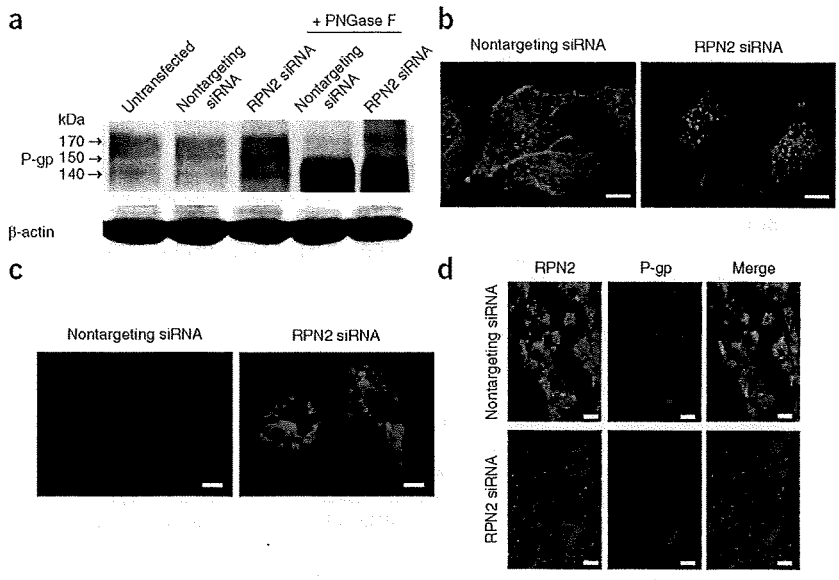

Figure 5 RPN2 siRNA regulates glycosylation of P-glycoprotein (P-gp). **(a)** Western blot analysis shows the glycosylation status of P-gp in MCF7-ADR cells 72 h after transfection of RPN2 siRNA or control nontargeting siRNA. Bands migrating at 170, 150 and 140 kDa represent mature, immature and unglycosylated forms of P-gp, respectively. **(b)** Immunofluorescence staining of P-gp on MCF7-ADR cell membrane surfaces. Cells were treated with RPN2 siRNA or nontargeting siRNA for 72 h. Scale bar, 5 μm. **(c)** Rhodamine-123 retention in MCF7-ADR cells 72 h after transfection with RPN2 siRNA or control nontargeting siRNA. Scale bar, 5 μm. **(d)** Localization of P-gp in tumors of MCF7-ADR in mice. Immunofluorescence staining of RPN2 (green) and P-gp (red) are shown. Nuclei are blue (DAPI). Merged images are also shown. Scale bar, 5 μm.

Fig. 5a,b online). Similar results were observed for other breast cancer tissues (**Supplementary Fig. 5c**).

Thus, these data provide a clear link between the glycosylation status of P-glycoprotein and RPN2 expression in drug-resistant breast cancer cells, and the disappearance of the membrane-bound P-glycoprotein leads to a reversal of the multidrug- resistant phenotype.

DISCUSSION

Cancer researchers today are confronted with how to best identify and select the next generation of molecular targets for oncology. An impressive array of potential new cellular targets, suitable for therapeutic intervention, has been revealed by the recent completion of the human genome sequencing project. Approaches as varied as transcription profiling, proteomics and the use of siRNAs are all being exploited in the race to select the most promising candidate drug targets. We tested the feasibility of using atelocollagen-mediated RNAi delivery *in vitro* and *in vivo* to obtain an unbiased evaluation on the efficacy of a specific siRNA related to drug resistance in human breast cancer. We show here that, among genes whose expression was elevated in nonresponders to docetaxel, the siRNA designed for *RPN2* significantly promoted docetaxel-dependent apoptosis and cell growth inhibition of MCF7-ADR human breast cancer cells that exhibit docetaxel resistance. A clinicopathological study showed that there is a significant association of *RPN2* expression with a pathologic response to docetaxel. Most notably, atelocollagen-mediated *in vivo* delivery of RPN2 siRNA significantly reduced the size of orthotopic MCF7-ADR tumors in mice given docetaxel.

In this study, we demonstrated that the atelocollagen delivery system markedly enhanced the efficiency of siRNA for the inhibition of RPN2 in mouse tumor models of human breast cancer. Because siRNA shows very low efficiency in gene silencing *in vivo*, various delivery methods, such as the use of plasmids and viral vectors encoding siRNA and the use of lipids, have been investigated. We have previously shown that the atelocollagen-mediated systemic delivery of siRNA might be a unique strategy for the inhibition of bone-metastatic prostate tumor growth[22]. The siRNA-atelocollagen complex is a nano-sized particle and is stable *in vitro* and *in vivo*[21,29]. Furthermore, we have previously confirmed that the atelocollagen complex shows low toxicity and low immunogenicity *in vivo*[23,24]. Thus, an atelocollagen-mediated local or systemic delivery system holds great potential for the practical application of gene suppression using siRNAs for cancer therapeutics.

Targeting of P-glycoprotein by small-molecular compounds, antibodies or both is an effective strategy to overcome multiple drug resistance in cancer[30]. Despite promising previous studies showing that the inhibition of P-glycoprotein by pharmacological means can sensitize drug-resistant cells, the ultimate goal of restoring drug sensitivity has met with limited success in clinical trials. Our results indicate that RPN2 is partly responsible for P-glycoprotein–mediated drug resistance in breast cancer and is involved in the regulation of the glycosylation status of P-glycoprotein. In fact, downregulation of *RPN2* restored drug retention, suggesting that P-glycoprotein function is inhibited via suppression of the glycosylation of P-glycoprotein in MCF7-ADR cells. *N*-glycosylation has been shown to contribute to the stability of the P-glycoproteins[31], and it has been reported that reduced glycosylation results in the disappearance of membrane-bound P-glycoprotein, which causes the loss of a multidrug-resistant phenotype[32]. Furthermore, multidrug-resistant cells are hypersensitive to the *N*-linked glycosylation inhibitor tunicamycin, which induces partial inhibition of the glycosylation of GLUT-1, a glucose transporter, and diminishes GLUT-1–mediated transport[33]. Because the amount of MDR1 mRNA was not significantly decreased in MCF7-ADR cells transduced with RPN2 siRNA, it is predicted that RPN2 inhibition may reduce the glycosylation of P-glycoprotein, thereby inducing perturbation of its subcellular localization, inhibition of its protein synthesis and/or acceleration of its degradation, with MCF7-ADR cells inevitably becoming hypersensitive response to docetaxel. In contrast, the RPN2 protein is part of an *N*-oligosaccharyl transferase complex that links to *N*-glycosylation ability; therefore, RPN2 inhibition could affect *N*-oligosaccharyl transferase function, resulting in impaired glycosylation of the P-glycoproteins. We speculate that RPN2 has a key role in drug-resistant tumor cells that overexpress P-glycoprotein and acts as a facilitator, stabilizing factor or both for *N*-glycosylation of P-glycoprotein. The coordinated expression of RPN2 and P-glycoprotein may participate in the mechanism of docetaxel resistance via the glycosylation status of P-glycoprotein.

However, one group has recently reported that the stability of P-glycoprotein is regulated by the ubiquitin-proteasome pathway in multidrug-resistant cancer cells[34]. Furthermore, the P-glycoprotein must be phosphorylated by protein kinase C (PKC) to effectively

function as a drug-efflux pump[35], which suggests that PKC is indirectly involved in the development of the multidrug-resistant phenotype. More recently, it was revealed that wild-type p53, a tumor suppressor, may resensitize soft tissue sarcoma to chemotherapeutic agents by reducing MDR1 phosphorylation via transcriptional repression of PKC expression[36]. There is no direct evidence of RPN2 involvement with the transcriptional repression of PKC. Other transporter proteins mediating drug resistance are the multidrug resistance–associated protein and ABCG2. Whether these different populations of multidrug resistance–associated protein family members and ABCG2 are affected by RPN2 has yet to be determined.

Recently, downregulation of multidrug resistance by the introduction of synthetic siRNAs has been reported[37,38]. However, only partial reversal of the drug-sensitive phenotype of the cells has been obtained. A possible explanation for this low inhibitory effect is that it was the result of a long half-life of P-glycoprotein[39] and the less efficient delivery of synthetic siRNAs into cells. Although the data are not shown, we compared the cell growth inhibition by synthetic RPN2 siRNA versus MDR1 siRNA in the presence of docetaxel *in vitro*. At the mRNA level, the downregulation of RPN2 and MDR1 obtained with the most efficient siRNA was 90% and 80%, respectively. These results indicate that cell growth inhibition was achieved by both siRNAs, although RPN2 siRNA showed a stronger growth inhibitory effect compared to MDR1 siRNA. Thus, though it is impossible at the moment to judge whether MDR1 or RPN2 is a more profitable target for overcoming drug resistance, RPN2 does provide a valuable clue for making multidrug-resistant breast cancer cells sensitive to anticancer drugs.

The continuing interest in apoptosis among cancer biologists has been strengthened by the hope that a molecular understanding of cell death will inform our understanding of cancer drug resistance. In fact, upregulation of antiapoptotic *Bcl2* family genes has been shown to be key in tumor malignancy and drug resistance[40,41]. Overexpression of exogenous Bcl-xL or Bcl-2 suppresses apoptosis[42,43]. In our study, knockdown of RPN2 by siRNA in MCF7-ADR cells selectively downregulated mRNA expression of Bcl-xL and Bcl-w (**Supplementary Fig. 6** online). These results suggest that RPN2 regulates Bcl-xL– and Bcl-w–mediated antiapoptosis and may be partly responsible for the docetaxel resistance of the MCF7-ADR cells. It has already been reported that apoptosis-based therapies[44], such as the downregulation of Bcl-xL expression, Bcl-w expression or both with antisense oligonucleotides, abolish tumorigenicity and enhance chemosensitivity in human malignant glioma cells[45–47]. In addition, Bcl-xL and Bcl-w are upregulated by nuclear factor-κB (NF-κB)[48]. Some chemotherapeutic agents, such as cisplatin and docetaxel, instantly induce the activation of NF-κB in cancer cells, and the cells become drug resistant[49]. In fact, we found that *RPN2* gene expression is also induced by docetaxel treatment of drug-sensitive MCF7 cells. Therefore, it would be useful to know whether RPN2 induces the downregulation of Bcl-xL and Bcl-w in MCF7-ADR cells by direct association with the NF-κB signaling pathway.

It is noteworthy that our findings using docetaxel-resistant human breast cancer cells are commonly found in other multiple cancers. Cisplatin-resistant human non–small cell lung carcinoma cells recover their sensitivity to cisplatin by knockdown of *RPN2* expression and die by apoptosis (Y.Y., K.H. and T.O., unpublished data). In addition, mouse mammary tumor cells resistant to docetaxel express mouse Rpn2, and inhibition of Rpn2 results in apoptotic cell death in the presence of docetaxel (**Supplementary Fig. 2e–g**). Therefore, RPN2 status is responsible for the drug-resistant nature of multiple cancer cell lines both in humans and in mice, and RPN2 expression may confer cross-resistance to a variety of anticancer drugs.

We previously reported that a group of redox genes is useful for the prediction of the clinical response to docetaxel in subjects with breast cancer[16]. Our current results indicate that the RPN2 mRNA level might serve as a predictor of the response to anticancer therapy rather than as a prognostic factor. The determination of the RPN2 mRNA level will be useful in the selection of subjects who are likely to benefit from adjuvant chemotherapy. Furthermore, our animal experiments suggest that treatment of subjects with a pharmacological agent that blocks RPN2 expression or function may induce a complete response to chemotherapeutic drugs. The *RPN2* gene may therefore represent a promising new target for RNAi therapeutics against multidrug-resistant tumors.

METHODS

Cell culture. Human mammary carcinoma cell lines, MCF7 cells and multidrug-resistant MCF7-ADR cells were provided by Shien-Lab, Medical Oncology, National Cancer Center Hospital of Japan. We cultured MCF7, MCF7-ADR and MDA-MB-231 (American Type Culture Collection) cells in RPMI 1640 (Gibco BRL) supplemented with 10% FBS (Gibco BRL) under 5% CO_2 in a humidified incubator at 37 °C. We cultured the mouse mammary tumor cell line EMT6/AR10.0 (European Collection of Cell Cultures), which shows docetaxel resistance, in MEM (EBSS) with 2 mM glutamine, 1% non essential amino acids and 10% FBS. The establishment of bioluminescent MCF7-ADR-Luc cells and docetaxel-resistant MDA-MB-231/MDR1 cells is described in **Supplementary Methods** online.

Design and synthesis of small interfering RNAs. We designed siRNAs and synthesized them with an siRNA duplex for each gene target (Dharmacon) for the preparation of an atelocollagen-based cell transfection array. The siRNA sequences are described in **Supplementary Methods.**

Atelocollagen-based cell transfection array. For RNAi-based functional screening, we prepared an atelocollagen-based cell transfection array, which enables reverse transfection of cells by atelocollagen-mediated gene transfer (**Supplementary Methods**). We performed live-cell luciferase assay for measurement of cell growth, and we performed caspase-7 assays with Apo-ONE Caspase-3/7 Assay Reagent (Promega) and Hoechst staining for apoptosis (**Supplementary Methods**).

Real-time reverse transcription PCR. We purified total RNA from cells and tumor tissues with an RNeasy Mini Kit and RNase-Free DNase Set (QIAGEN) and produced cDNAs with an ExScript RT reagent Kit (Takara). We then subjected cDNA samples to real-time PCR with SYBR Premix Ex Taq (Takara) and specific primers (**Supplementary Methods**). We carried out the reactions in a LightCycler (Roche Diagnostics). We normalized gene expression levels by *HPRT1* or *ACTB*. The cell-direct quantitative RT-PCR method is described in the **Supplementary Methods.**

Atelocollagen-mediated RPN2 small interfering RNA delivery *in vivo*. We performed mouse experiments in compliance with the guidelines of the Institute for Laboratory Animal Research at the National Cancer Center Research Institute of Japan. We used 4-week-old female athymic nude mice (CLEA Japan) to generate an experimental orthotopic breast cancer model. We injected 1.0×10^7 MCF7-ADR cells or MDA-MB-231/MDR1 cells suspended in 100 μl sterile PBS into the fat pad. When the tumor grew to approximately 5 mm in diameter, we injected mice with 200 μl of siRNA-atelocollagen by intratumoral injection. Preparation of the siRNA-atelocollagen complex is described in the **Supplementary Methods.** Simultaneously, we injected docetaxel i.p. into mice. We harvested tumor tissues for analysis of RPN2 mRNA and RPN2 protein at 24 h and 72 h after treatment, respectively.

TUNEL technique. We harvested tumor tissues 72 h after administration of siRNA and prepared frozen sections. We then performed TUNEL staining with an *in situ* Cell Death Detection Kit, Fluorescein (Roche Diagnostics), according to the manufacturer's protocol. We stained the nuclei with DAPI. We

determined the number of fluorescein-positive cells in three microscopic fields of each section by fluorescence microscopy.

Docetaxel disposition in tumors. We studied drug disposition of docetaxel in tumors in mice by HPLC with ultraviolet detection at 225 nm after solid-liquid extraction as described elsewhere[50]. Eleven hours after i.p. administration of 20 mg kg^{-1} docetaxel, we harvested the tumors treated with siRNA-atelocollagen complex and then analyzed the docetaxel abundance in the tumor.

Transfection of small interfering RNA. We carried out transfection of MCF7-ADR and EMT6/AR10.0 cells with siRNA using DharmaFECT 1 (Dharmacon) and TransIT-TKO (Mirus), respectively, according to the manufacturers' protocol (**Supplementary Methods**).

Antibodies. We used RPN2-specific antibody (H300, Santa Cruz Biotechnology) and MDR-specific antibody (G-1, Santa Cruz Biotechnology). We visualized staining with Alexa 488 or Alexa 594 (Molecular Probes). We used fluorescence microscopy or confocal fluorescence microscopy (Olympus) for observation of immunofluorescence-stained cells. The procedures of western blotting and immunofluorescence staining are described in the **Supplementary Methods**.

Rhodamine-123 retention assay. We washed cells once with prewarmed Opti-MEM I medium (37 °C, Gibco BRL) and incubated the cells for 30 min at 37 °C in the Opti-MEM I medium containing 10 μM rhodamine-123. We then removed the rhodamine-123 solution from the extracellular medium and washed the cells twice with Opti-MEM I medium. We observed the cells for fluorescence of rhodamine-123 under fluorescence microscopy.

Human samples. The study protocol for clinical samples (results presented in **Table 1**) was approved by the Institutional Review Board of Osaka University Medical School, and written informed consent was obtained from each subject (**Supplementary Note**).

Statistical analyses. We conducted statistical analysis by analysis of variance with the Student's *t*-test. We considered a *P* value of 0.05 or less as a significant difference.

Note: Supplementary information is available on the Nature Medicine website.

ACKNOWLEDGMENTS

Human mammary carcinoma cell lines, MCF7 cells and multidrug-resistant MCF7-ADR cells were provided by Shien-Lab, Medical Oncology, National Cancer Center Hospital of Japan. We gratefully thank S. Noguchi for the initiation of the whole project and for helpful discussion. We also thank H. Inaji, K. Yoshioka and K. Itoh for their kind assistance; J. Miyazaki (Osaka University) for the kind gift of CAG promoter; and A. Inoue and M. Wada for their excellent technical work. This work was supported in part by a grant-in-aid for the Third-Term Comprehensive 10-Year Strategy for Cancer Control of Japan; a grant-in-aid for Scientific Research on Priority Areas Cancer from the Japanese Ministry of Education, Culture, Sports, Science and Technology; and the Program for Promotion of Fundamental Studies in Health Sciences of the National Institute of Biomedical Innovation of Japan.

AUTHOR CONTRIBUTIONS

K.H. performed the experimental work, data analysis and writing of the first draft of the manuscript. K.K. and T.O. selected the initial set of genes subjected to the screening. K.I.-K., K.K., T.Y. and T.O. participated in the conception, design and coordination of the study. F.T. and Y.Y. performed siRNA delivery *in vivo* and helped with data analysis. K.N. provided drug-resistant cell lines. S.N. provided delivery molecules. The manuscript was finalized by T.O. with the assistance of all authors.

Published online at http://www.nature.com/naturemedicine/
Reprints and permissions information is available online at http://npg.nature.com/reprintsandpermissions/

1. Kaufmann, M. *et al.* International expert panel on the use of primary (preoperative) systemic treatment of operable breast cancer: review and recommendations. *J. Clin. Oncol.* **21**, 2600–2608 (2003).
2. Gradishar, W.J. *et al.* Neoadjuvant docetaxel followed by adjuvant doxorubicin and cyclophosphamide in patients with stage III breast cancer. *Ann. Oncol.* **16**, 1297–1304 (2005).
3. Formenti, S.C. *et al.* Preoperative twice-weekly paclitaxel with concurrent radiation therapy followed by surgery and postoperative doxorubicin-based chemotherapy in locally advanced breast cancer: A phase I/II trial. *J. Clin. Oncol.* **21**, 864–870 (2003).
4. Engels, F.K., Sparreboom, A., Mathot, R.A. & Verweij, J. Potential for improvement of docetaxel-based chemotherapy: a pharmacological review. *Br. J. Cancer* **93**, 173–177 (2005).
5. Crown, J., O'Leary, M. & Ooi, W.S. Docetaxel & paclitaxel in the treatment of breast cancer: a review of clinical experience. *Oncologist* **9**, 24–32 (2004).
6. Jones, S.E. *et al.* Randomized phase III study of docetaxel compared with paclitaxel in metastatic breast cancer. *J. Clin. Oncol.* **23**, 5542–5551 (2005).
7. Bonneterre, J. *et al.* Efficacy and safety of docetaxel (Taxotere) in heavily pretreated advanced breast cancer patients: the French compassionate use programme experience. *Eur. J. Cancer* **35**, 1431–1439 (1999).
8. Gottesman, M.M., Pastan, I. & Ambudkar, S.V. P-glycoprotein and multidrug resistance. *Curr. Opin. Genet. Dev.* **6**, 610–617 (1996).
9. Duan, Z., Brakora, K.A. & Seiden, M.V. Inhibition of ABCB1 (MDR1) and ABCB4 (MDR3) expression by small interfering RNA and reversal of paclitaxel resistance in human ovarian cancer cells. *Mol. Cancer Ther.* **3**, 833–838 (2004).
10. Leslie, E.M., Deeley, R.G. & Cole, S.P. Toxicological relevance of the multidrug resistance protein 1, MRP1 (ABCC1) and related transporters. *Toxicology* **167**, 3–23 (2001).
11. Renes, J., de Vries, E.G., Jansen, P.L. & Muller, M. The (patho)physiological functions of the MRP family. *Drug Resist. Updat.* **3**, 289–302 (2000).
12. Leonessa, F. & Clarke, R. ATP binding cassette transporters and drug resistance in breast cancer. *Endocr. Relat. Cancer* **10**, 43–73 (2003).
13. Lin, J.C., Chang, S.Y., Hsieh, D.S., Lee, C.F. & Yu, D.S. The association of Id-1, MIF and GSTpi with acquired drug resistance in hormone independent prostate cancer cells. *Oncol. Rep.* **13**, 983–988 (2005).
14. Galimberti, S., Testi, R., Guerrini, F., Fazzi, R. & Petrini, M. The clinical relevance of the expression of several multidrug-resistant–related genes in patients with primary acute myeloid leukemia. *J. Chemother.* **15**, 374–379 (2003).
15. Burg, D., Riepsaame, J., Pont, C., Mulder, G. & van de Water, B. Peptide-bond modified glutathione conjugate analogs modulate GSTpi function in GSH-conjugation, drug sensitivity and JNK signaling. *Biochem. Pharmacol.* **71**, 268–277 (2006).
16. Iwao-Koizumi, K. *et al.* Prediction of docetaxel response in human breast cancer by gene expression profiling. *J. Clin. Oncol.* **23**, 422–431 (2005).
17. Kim, S.J. *et al.* High thioredoxin expression is associated with resistance to docetaxel in primary breast cancer. *Clin. Cancer Res.* **11**, 8425–8430 (2005).
18. Kato, K. Adaptor-tagged competitive PCR: a novel method for measuring relative gene expression. *Nucleic Acids Res.* **25**, 4694–4696 (1997).
19. Honma, K. *et al.* Atelocollagen-based gene transfer in cells allows high-throughput screening of gene functions. *Biochem. Biophys. Res. Commun.* **289**, 1075–1081 (2001).
20. Honma, K., Miyata, T. & Ochiya, T. The role of atelocollagen-based cell transfection array in high-throughput screening of gene functions and in drug discovery. *Curr. Drug Discov. Technol.* **1**, 287–294 (2004).
21. Minakuchi, Y. *et al.* Atelocollagen-mediated synthetic small interfering RNA delivery for effective gene silencing *in vitro* and *in vivo*. *Nucleic Acids Res.* **32**, e109 (2004).
22. Takeshita, F. *et al.* Efficient delivery of small interfering RNA to bone-metastatic tumors by using atelocollagen *in vivo*. *Proc. Natl. Acad. Sci. USA* **102**, 12177–12182 (2005).
23. Ochiya, T. *et al.* New delivery system for plasmid DNA *in vivo* using atelocollagen as a carrier material: the Minipellet. *Nat. Med.* **5**, 707–710 (1999).
24. Ochiya, T., Nagahara, S., Sano, A., Itoh, H. & Terada, M. Biomaterials for gene delivery: atelocollagen-mediated controlled release of molecular medicines. *Curr. Gene Ther.* **1**, 31–52 (2001).
25. Crimaudo, C., Hortsch, M., Gausepohl, H. & Meyer, D.I. Human ribophorins I and II: the primary structure and membrane topology of two highly conserved rough endoplasmic reticulum-specific glycoproteins. *EMBO J.* **6**, 75–82 (1987).
26. Kelleher, D.J., Kreibich, G. & Gilmore, R. Oligosaccharyltransferase activity is associated with a protein complex composed of ribophorins I and II and a 48 kd protein. *Cell* **69**, 55–65 (1992).
27. Kelleher, D.J. & Gilmore, R. An evolving view of the eukaryotic oligosaccharyltransferase. *Glycobiology* **16**, 47R–62R (2006).
28. Loo, T.W., Bartlett, M.C. & Clarke, D.M. The dileucine motif at the COOH terminus of human multidrug resistance P-glycoprotein is important for folding but not activity. *J. Biol. Chem.* **280**, 2522–2528 (2005).
29. Ochiya, T., Honma, K., Takeshita, F. & Nagahara, S. Atelocollagen-mediated drug discovery technology. *Expert Opin. Drug Discov.* **2**, 159–167 (2007).
30. Tsuruo, T. *et al.* Molecular targeting therapy of cancer: drug resistance, apoptosis and survival signal. *Cancer Sci.* **94**, 15–21 (2003).
31. Schinkel, A.H., Kemp, S., Dolle, M., Rudenko, G. & Wagenaar, E. *N*-glycosylation and deletion mutants of the human MDR1 P-glycoprotein. *J. Biol. Chem.* **268**, 7474–7481 (1993).
32. Kramer, R. *et al.* Inhibition of *N*-linked glycosylation of P-glycoprotein by tunicamycin results in a reduced multidrug resistance phenotype. *Br. J. Cancer* **71**, 670–675 (1995).
33. Bentley, J., Quinn, D.M., Pitman, R.S., Warr, J.R. & Kellett, G.L. The human KB multidrug-resistant cell line KB-C1 is hypersensitive to inhibitors of glycosylation. *Cancer Lett.* **115**, 221–227 (1997).
34. Zhang, Z., Wu, J.Y., Hait, W.N. & Yang, J.M. Regulation of the stability of P-glycoprotein by ubiquitination. *Mol. Pharmacol.* **66**, 395–403 (2004).

35. O'Brian, C.A., Ward, N.E., Stewart, J.R. & Chu, F. Prospects for targeting protein kinase C isozymes in the therapy of drug-resistant cancer—an evolving story. *Cancer Metastasis Rev.* **20**, 95–100 (2001).
36. Zhan, M. *et al.* Transcriptional repression of protein kinase Cα via Sp1 by wild type p53 is involved in inhibition of multidrug resistance 1 P-glycoprotein phosphorylation. *J. Biol. Chem.* **280**, 4825–4833 (2005).
37. Nieth, C., Priebsch, A., Stege, A. & Lage, H. Modulation of the classical multidrug resistance (MDR) phenotype by RNA interference (RNAi). *FEBS Lett.* **545**, 144–150 (2003).
38. Wu, H., Hait, W.N. & Yang, J.M. Small interfering RNA–induced suppression of MDR1 (P-glycoprotein) restores sensitivity to multidrug-resistant cancer cells. *Cancer Res.* **63**, 1515–1519 (2003).
39. Muller, C., Laurent, G. & Ling, V. P-glycoprotein stability is affected by serum deprivation and high cell density in multidrug-resistant cells. *J. Cell. Physiol.* **163**, 538–544 (1995).
40. Pommier, Y., Sordet, O., Antony, S., Hayward, R.L. & Kohn, K.W. Apoptosis defects and chemotherapy resistance: molecular interaction maps and networks. *Oncogene* **23**, 2934–2949 (2004).
41. Sordet, O., Khan, Q.A., Kohn, K.W. & Pommier, Y. Apoptosis induced by topoisomerase inhibitors. *Curr. Med. Chem. Anticancer Agents* **3**, 271–290 (2003).
42. Schott, A.F., Apel, I.J., Nunez, G. & Clarke, M.F. Bcl-XL protects cancer cells from p53-mediated apoptosis. *Oncogene* **11**, 1389–1394 (1995).
43. Walczak, H., Bouchon, A., Stahl, H. & Krammer, P.H. Tumor necrosis factor-related apoptosis-inducing ligand retains its apoptosis-inducing capacity on Bcl-2– or Bcl-xL–overexpressing chemotherapy-resistant tumor cells. *Cancer Res.* **60**, 3051–3057 (2000).
44. Reed, J.C. Apoptosis-based therapies. *Nat. Rev. Drug Discov.* **1**, 111–121 (2002).
45. Lytle, R.A., Jiang, Z., Zheng, X. & Rich, K.M. BCNU down-regulates anti-apoptotic proteins Bcl-xL and Bcl-2 in association with cell death in oligodendroglioma-derived cells. *J. Neurooncol.* **68**, 233–241 (2004).
46. Jiang, Z., Zheng, X. & Rich, K.M. Down-regulation of Bcl-2 and Bcl-xL expression with bispecific antisense treatment in glioblastoma cell lines induce cell death. *J. Neurochem.* **84**, 273–281 (2003).
47. Guensberg, P. *et al.* Bcl-xL antisense oligonucleotides chemosensitize human glioblastoma cells. *Chemotherapy* **48**, 189–195 (2002).
48. Tran, N.L. *et al.* The tumor necrosis factor–like weak inducer of apoptosis (TWEAK)-fibroblast growth factor–inducible 14 (Fn14) signaling system regulates glioma cell survival via NFκB pathway activation and BCL-XL/BCL-W expression. *J. Biol. Chem.* **280**, 3483–3492 (2005).
49. Li, Y. *et al.* Inactivation of nuclear factor κB by soy isoflavone genistein contributes to increased apoptosis induced by chemotherapeutic agents in human cancer cells. *Cancer Res.* **65**, 6934–6942 (2005).
50. Vergniol, J.C., Bruno, R., Montay, G. & Frydman, A. Determination of Taxotere in human plasma by a semi-automated high-performance liquid chromatographic method. *J. Chromatogr.* **582**, 273–278 (1992).

Establishment and molecular profiling of a novel human pancreatic cancer panel for 5-FU

Kazuyoshi Yanagihara,[1,4] Misato Takigahira,[1] Hiromi Tanaka,[1] Tokuzo Arao,[2] Yasuyuki Aoyagi,[3] Tatsuya Oda,[3] Atsushi Ochiai[3] and Kazuto Nishio[2]

[1]Central Animal Laboratory, National Cancer Center Research Institute, Tokyo, Tsukiji 5-1-1, Chuo-ku, Tokyo 104-0045; [2]Department of Genome Biology, Kinki University School of Medicine, Ohno-Higashi 377-2, Osaka-Sayama, Osaka 589-8511; [3]Pathology Division, Research Center for Innovative Oncology, National Cancer Center Research at Kashiwa, Kashiwanoha 6-5-1, Kashiwa, Chiba 277-8577, Japan

(Received April 30, 2008/Revised May 27, 2008/Accepted May 27, 2008/Online publication August 7, 2008)

Ten novel human pancreatic carcinoma cell lines (Sui65 through Sui74) were established from a transplantable pancreatic carcinoma cell line. All the cell lines resembled the original clinical carcinoma in terms of the morphological and biological features, presenting with genetic alterations such as point mutations of *K-ras* and *p53*, attenuation or lack of *SMAD4* and *p16* and other relevant cellular characteristics. Using this panel, we evaluated the effects of 5-FU in suppressing the proliferation of pancreatic carcinoma cells. When tested *in vitro*, although Sui72 was highly susceptible to 5-FU, the other cell lines were found to be resistant to the drug. When Sui72 and Sui70 were implanted subcutaneously in SCID mice followed by treatment with 5-FU, the drug was found to be effective against Sui72 but not Sui70, consistent with the results *in vitro*. In order to identify the molecular determinant for high sensitivity of Sui72 to 5-FU, we examined the mRNA expression levels of the metabolic enzymes of 5-FU. Decreased expression of DPYD was observed in Sui72 as compared with other cell lines (0.1 *versus* 0.6 ± 0.5, 0.1-fold).

It is believed that the novel cell lines established in the present study will be useful for analyzing the pattern of progression of pancreatic cancer and for evaluating the efficacy of anticancer agents. (*Cancer Sci* 2008; 99: 1859–1864)

Pancreatic cancer is an intractable cancer with a prognosis poorer than that of any other cancer of the gastrointestinal tract. In Japan, the 5-year survival rate of patients with pancreatic cancer is 5.5%, which is extremely low as compared with that of patients with colorectal cancer (64.6%), gastric cancer (58.8%) or even hepatic cancer (17.1%).[1,2] The number of patients with this cancer has been increasing significantly in recent years, and the mean life expectancy of patients with this cancer is only about 1.5 years. Pancreatic cancer, often characterized by pain, jaundice and digestive dysfunction, causes much pain and stress to the patient. These characteristics make this cancer an important open issue in medicine and healthcare. Currently, no valid clinical means are available for the prevention, diagnosis or treatment of this cancer. Treatment of pancreatic cancer with local therapy alone, that is surgical resection and radiotherapy, has limitations, and chemotherapy needs to be considered.[2] In the past, various adjuvant chemotherapy regimes, primarily based on 5-FU, have been attempted;[3–5] however, no effective therapy has as yet been established for pancreatic cancer.

In recent years, close attention has been paid to the development of cancer treatment methods based on information about the molecular mechanism of onset and progression of cancer.[2,6,7] Thus, exploration of molecular markers and target molecules for treatment is expected to play a key role in cancer management. For this kind of preclinical research, in particular, for evaluation of the efficacy of molecule-targeted drugs, the development of a panel of cultured cells derived from clinical cancer specimens is indispensable. To date, a number of cell lines derived from human pancreatic cancer have been established[8–15] and have contributed greatly to advancing cancer research[15,16] in terms of analysis of biological features and evaluation of the efficacy of anticancer agents. However, after multiple passages, some of these cell lines lose their original features (e.g. histopathological characteristics of the tumor formed after implantation, etc.).

The present study was undertaken to establish 10 novel cell lines derived from human pancreatic carcinoma that would reliably reflect the clinical features of pancreatic carcinoma. We investigated the proliferative characteristics and genetic alterations in these cell lines, then, using the panel of cell lines, we evaluated the efficacy of conventional 5-FU-based chemotherapy against pancreatic cancer and attempted to elucidate the determinants of sensitivity of these pancreatic cancer cell lines to 5-FU-based anticancer agents.

Materials and Methods

Establishment of the cell lines. All the cell lines were established *in vitro* from xenotransplantable tumors (taco series) originating from primary or metastatic human pancreatic cancer (Table 1) (T. Oda and A. Ochiai, unpublished data). The cell lines were established by s.c. back transplantation of the primary tumor for the 8th transplant generation, then tumors were removed for *in vitro* cultivation. Fresh tumor specimens obtained under sterile conditions were washed five times in Roswell Park Memorial Institute medium (RPMI)-1640 containing streptomycin (500 μg/mL) and penicillin (500 IU/mL). The tumor tissue specimens were trimmed of fat and necrotic materials and minced with a scalpel. The tissue pieces were transferred together with Dulbecco's Modified Eagle Medium (DMEM) + Ham's F12 + 5% fetal bovine serum (FBS), at 10–15 fragments per dish, to 60-mm culture dishes.[17] The dishes were left undisturbed for 24 h at 37°C in a 5% CO_2/95% air atmosphere. The medium was composed of Dulbecco's modified Eagle's medium (DMEM)/Ham's F12 medium (1:1) supplemented with 5% fetal bovine serum (FBS; Gibco, Grand Island, NY, USA), 100 IU/mL penicillin G sodium, and 100 mg/mL streptomycin sulfate (Immuno-Biological Laboratories [IBL], Fujioka, Japan). After 48 h, the medium was replaced by RPMI-1640 medium (IBL, Fujioka, Japan) supplemented with 10% FBS, 100 IU/mL penicillin G sodium and 100 mg/mL streptomycin sulfate. The dishes containing the tissue fragments were observed weekly under an inverted phase microscope. The dishes were initially trypsinized (0.05% trypsin and 0.02% ethylenediametetraacetic acid [EDTA]) to selectively remove overgrowing fibroblasts. In addition, we also attempted to remove the fibroblasts mechanically and transfer only the tumor cells. Half of the medium was changed every 4–6 days. The cultures were first split after 3–8 months of cultivation, and the

[4]To whom correspondence should be addressed. E-mail: kyanagih@ncc.go.jp
T. Oda and Y. Aoyagi are currently at HBP Surgery, Tsukuba University, Clinical Medicine, Japan.
Abbreviations: i.p., intraperitoneal; s.c., subcutaneous; TPA, tissue polypeptide antigen; 5-FU, 5-fluorouracil; SCID, severe combined immunodeficiency.

doi: 10.1111/j.1349-7006.2008.00896.x

Table 1. Establishment of ten human pancreatic cancer cell lines from the xenotransplantable tumors

Cell line	Source	Origin		Histology
	xenograft tumor	Age/sex	Source (TNM)	
Sui65	taco-1	63/F	Peritoneum (metastatic focus)	Tubular adenocarcinoma c/w meta
Sui66	taco-2	74/M	Pancreas	Tubular adenocarcinoma
Sui67	taco-4	73/F	Pancreas	Tubular adenocarcinoma
Sui68	taco-5	53/M	Pancreas	Adenocarcinoma
Sui69	taco-6	54/M	Pancreas	Tubular adenocarcinoma
Sui70	taco-7	53/M	Pancreas	Adenocarcinoma
Sui71	taco-12	65/M	Liver (metastatic focus)	Adenocarcinoma c/w meta
Sui72	taco-13	76/F	Pancreas	Tubular adenocarcinoma
Sui73	taco-15	65/F	Pancreas	Tubular adenocarcinoma
Sui74	taco-16	72/F	Pancreas	Adenocarcinoma

cells were passaged thereafter at a 1:10 or 1:20 ratio.[18] They were then judged, established and designated (Table 1). All of the cell lines were routinely tested for *Mycoplasma* using a PCR *Mycoplasma* Detection kit (Takara, Kyoto, Japan), and no contamination was detected. This study was conducted in accordance with the Declaration of Helsinki. Informed consent was obtained from all of the patients from whom the tumor specimens were obtained. The study protocol was approved by the institutional review board of the National Cancer Center (approved number: 17–43).

Animal experimentation. The animal experiment protocols were approved by the Committee for Ethics in Animal Experimentation, and the experiments were conducted in accordance with the Guideline for Animal Experiments of the National Cancer Center. Female SCID mice (C.B.17/Icr Jcl-scid) were purchased from CLEA Japan (Tokyo, Japan), and maintained under specific-pathogen-free conditions. Six- to 8-week-old mice were used for this experiment. The mice were housed in filter-protected cages and reared on sterile water. The ambient light was controlled to provide regular 12-h light : 12-h dark cycles.

Western blot analysis. *SMAD4* and *p16* expression was examined in all the cell lines using Western blotting.[19] An osteosarcoma (SaOs2) and a human embryonic kidney (293) cell line were used as positive controls for *p16* and *SMAD4*, respectively. Monoclonal mouse antihuman antibodies to *DPC4/Smad 4* (cloneB8, Santa Cruz Biotechnology, Santa Cruz, CA, USA) and to *p16* (clone G175-405, PharMingen, San Diego, CA, USA) were used.

Therapeutic studies with 5-fluorouracil (5-FU). S.C. implantation of 5×10^5 cultured cells suspended in 0.1 mL RPMI-1640 medium was conducted in 6-week-old female SCID mice. To evaluate the antitumor activity, 3 days after the tumor cell implantation, the mice were divided into three groups of six mice each according to the tumor volume on Day 0. The experimental mice were divided into a control group that received vehicle alone (saline), and experimental groups that received i.p. inoculation of different doses of the drug (50 and 100 mg/kg/head). On Days 3, 10 and 17, tumor-bearing mice received an i.p. injection of 5-FU. 5-FU was purchased from Sigma (St. Louis, MO, USA) and dissolved in saline before being injected. Tumor growth was measured weekly, in terms of the tumor diameter, with calipers. At appropriate intervals, or when moribund, the mice were sacrificed and the tissues were examined macroscopically for metastasis in various organs and then processed for histological examination, as described previously.[20]

Direct sequencing. Samples from the cell lines were analyzed for the presence of mutations in exon 1 of the K-*ras* (Kirsten rat sarcoma-2 viral oncogene homolog) gene and exons 5–8 of the p53 gene by direct sequencing of the PCR-amplified DNA fragments. PCR and direct sequencing were performed as described previously[21] using minor modifications.

Real-time reverse-transcription polymerase chain reaction. RNA derived from each cell line was converted to complementary DNA using a GeneAmp RNA PCR Core kit (Applied Biosystems, Foster City, CA, USA). Real-time reverse transcription–polymerase chain reaction (RT-PCR) were performed using Power SYBR Green PCR Master Mix (Applied Biosystems) and the 7900HT Fast Real-time PCR system (Applied Biosystems). The PCR conditions were as follows: one cycle of denaturation at 95°C for 10 min, followed by 40 cycles at 95°C for 15 s and 60°C for 60 s. Obtained data was normalized relative to glyceraldehyde-3-phosphate dehydrogenase (GAPD) expression. The following primers were used: DHFR-FW: 5′-GCA AAT AAA GTA GAC ATG GTC TGG A-3′; DHFR-RW: 5′-AGT TTA AGA TGG CCT GGG TGA-3′; FPGS-FW: 5′-TCT GCC CTA ACC TGA CAG AGG TG-3′; FPGS-RW: 5′-TCG TCC AGG TGG TTC CAG TG-3′; TP-FW: 5′-GAG GCA CCT TGG ATA AGC TGG A-3′; TP-RW: 5′-GCT GTC ACA TCT CTG GCT GCA TA-3′; UPP1-FW: 5′-GTA CTA TGC CCG GTG CTC CAA C-3′; UPP1-RW: 5′-CTC TGC CTT GAA GCA GGA ATC CA-3′; PRPS1-FW: 5′-AAC GCA TGC TTT GAG GCA GTA GTA G-3′; PRPS1-RW: 5′-CTG ATG GCT TCT GCA AGG ATC ATA-3′; DPYD-FW: 5′-CAA CGT AGA GCA AGT TGT GGC TAT G-3′; DPYD-RW: 5′-AGT CGA CAA TAG GGC AAA CAC TGA-3′; TYMS-FW: 5′-ATC ATC ATG TGC GCT TGG AAT C-3′; TYMS-RW: 5′-TGT TCA CCA CAT AGA ACT GGC AGA G-3′; OPRT-FW: 5′-CTG GCT CCC GAG TAA GCA TGA-3′; OPRT-RW: 5′-CTG CTG AGA TTA TGC CAC GAC CTA-3′; TK1-FW: 5′-ATT CTC GGG CCG ATG TTC TC-3′; TK1-RW: 5′-GCG AGT GTC TTT GGC ATA CTT GA-3′; MTHFR-FW: 5′-GGA CAC TAC CTC ACC TGC CAG TAT C-3′; MTHFR-RW: 5′-CCA GAA GCA GTT AGT TCT GAC ACC A-3′; NP-FW: 5′-CAA CCT ACC TGG TTT CAG TGG TCA-3′; NP-RW: 5′-CCG GTC GTA GGC ATC AGA CA-3′; UCK2-FW: 5′-TTC GTC AAG CCT GCC TTT GAG-3′; UCK2-RW: 5′-TGG ATG TGC TGC ACG ATG AG-3′; GAPD-FW: 5′-GCA CCG TCA AGG CTG AGA AC-3′; GAPD-RW: 5′-ATG GTG GTG AAG ACG CCA GT-3′.

Results

Establishment and characterization of pancreatic cancer cell lines. Ten cell lines derived from human pancreatic cancers (Sui65, Sui66, Sui67, Sui68, Sui69, Sui70, Sui71, Sui72, Sui73 and Sui74) were newly established in the present study (Table 1). All the cell lines formed mono-layered sheets with clustering on confluence (Fig. 1 upper column). These cell lines exhibited the typical morphologic features of epithelial cells, characterized by sheets of polygonal cells in a pavement-like arrangement. The Sui65, 67, 68, 70 and 71 cell lines were found to secrete carbohydrate antigen19-9 (CA19-9), the concentration of which in the culture supernatants varied from 69 to 450 units/mL (Table 2). Production of TPA was also detected from all of the cell lines. The doubling times of the cell lines varied from approximately 20.8 to 55.2 h in the RPMI-1640 medium

doi: 10.1111/j.1349-7006.2008.00896.x

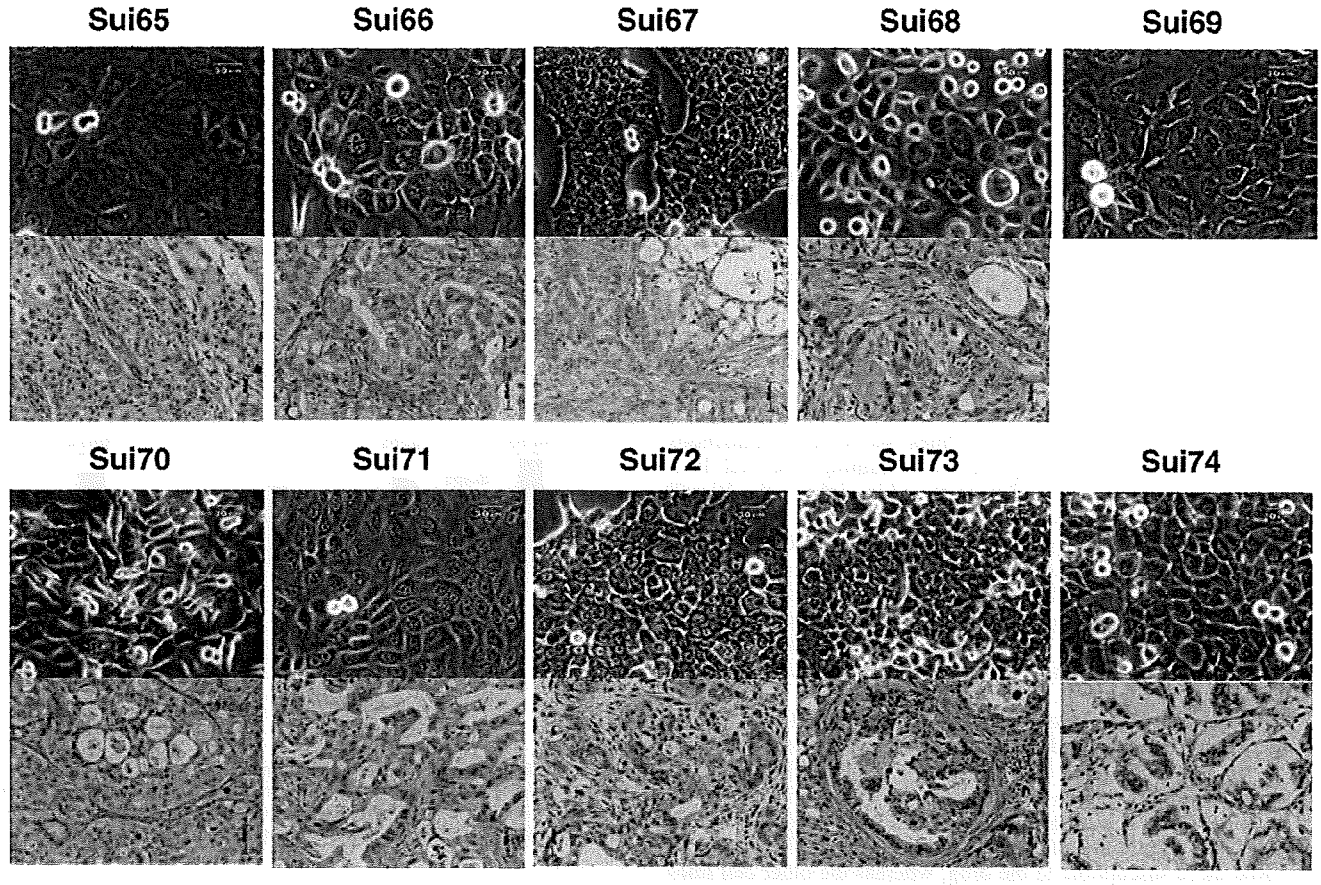

Fig. 1. Phase-contrast micrographs of the 10 established cell lines in this study (Sui65-Sui74) at the 25–30th passage (upper column). Original magnification, ×200. Histological section of a tumor established by s.c. injection of one of the cell lines into a SCID mouse (lower column). HE Stain, ×400.

Table 2. Biological characterization of newly established human pancreatic cancer cell lines

Cell line	Histological typing[†]		Growth[‡]				Tumor marker[§]			
	Original	Xenografts	Pattern	in CDM	in Agar	DT (h)	CEA ng/mL	CA19-9 u/mL	TPA u/L	CA125 u/mL
Sui65	Tub.ad.	Mod.tub.ad.	M	+	+	48.6	<0.5	69	2600	32.2
Sui66	Tub.ad.	Mod./well.	M	+	+	41.2	1.2	<6	1800	2.2
Sui67	Tub.ad.	Poor.tub.ad.	M	+	+	35.1	2.6	420	1600	1.5
Sui68	Ad.	Poor./mod.	M	+	+	43.3	5.1	450	980	3.2
Sui69	Tub.ad.	(–)	M	–	–	55.2	0.6	<6	2200	<1.0
Sui70	Ad.	Mod.tub.ad.	M	+	+	20.8	<0.5	290	14 000	7.5
Sui71	Ad.	Well.tub.ad.	M	+	+	24.1	<0.5	170	7100	9.3
Sui72	Tub.ad.	Mod.tub.ad. Sarcoma	M	+	+	27.8	31.6	<6	4400	<1.0
Sui73	Tub.ad.	Well./mod.	M	+	+	23.5	<0.5	<6	2400	1.5
Sui74	Ad.	Mucinos ca.	M	+	+	47.5	<0.5	<6	1800	13.5

[†]The tumorigenicity of the cell lines were tested by s.c. injection of 5×10^5 cultured cells suspended in 0.1 mL RPMI-1640 medium into mice. Histological typing of the pancreatic cancer was conducted in accordance with the 'General Rules for the Study of Pancreatic Cancer (1993)', as tub (tubular adenocarcinoma), or Muci. ca. (Mucinous carcinoma).
[‡]M, monolayer; CDM, composed of Dulbecco's modified Eagle's medium (DMEM)/Ham's F-12 (1:1) medium supplemented with 0.05% bovine serum albumin (BSA); +, positive; –, negative; DT, doubling time.
The doubling time of each line was determined as described previously.[20]
[§]Secretion of CEA, CA19-9, TPA and CA125 was tested by radioimmunoassay and immunoradioassay at SRL Laboratories (Tokyo, Japan).

supplemented with 10% FBS. When injected s.c., all of the cultured cell lines established from human pancreatic cancers, except for Sui69, survived and showed tumorigenicity (Fig. 1, lower column). These biological properties are summarized in Table 2. All the tumorigenic cell lines were also found to be strictly anchorage independent (60–90% efficiency).

Genetic alterations in the established pancreatic cancer cell lines. The results are summarized in Table 3. *K-ras* mutations were observed in eight of the 10 cell lines (80%). Activating mutations were detected in the 2nd base of codon 12 of *k-ras* in eight cell lines. The mutations were G-to-A transitions (GGT to GAT, Gly to Asp) in five cell lines, G-to-T transversions (GGT

Table 3. Molecular alterations of k-ras, p53, SMAD4 and P16 genes in newly established human pancreatic cancer cell lines

Cell line	Gene mutation				Gene expression	
	k-ras		p53		SMAD4/DPC4	p16
Sui65	codon12	GGT(Gly) → GAT(Asp)	codon248	CGG(Arg) → CAG(Gln)	–	–
Sui66	codon12	GGT(Gly) → GAT(Asp)	codon133	ATG(Met) → AAG(Lys)	+	–
Sui67	codon12	GGT(Gly) → GAT(Asp)	codon248	CGG(Arg) → TGG(Trp)	–	+
Sui68	codon12	GGT(Gly) → GAT(Asp)	codon245	GGC(Gly) → AGC(Ser)	+	–
Sui69	codon12	GGT(Gly) → GTT(Val)	codon175	CGC(Arg) → CAC(His)	–	–
Sui70	codon12	GGT(Gly) → GTT(Val)	codon175	CGC(Arg) → CAC(His)	–	–
Sui71	codon12	GGT(Gly) → GAT(Asp)	codon253	ACC(Thr) → CCC(Pro)	–	+
Sui72	Wt		codon135	TGC(Cys) → TAC(Tyr)	+	–
Sui73	Wt		Wt		+	–
Sui74	codon12	GGT(Gly) → CGT(Arg)	Wt	–	+	

to GTT, Gly to Val) in two cell lines and G-to-G transitions (GGT to GGT, Gly to Arg) in the remaining one cell line. Inactivating mutations of *p53* were found in eight of the 10 cell lines (80%), and included missense mutations.

Next, *SMAD4/DPC4* gene expression was checked by Western blot analysis. Marked expression of this gene was observed in Sui66 and Sui73, while the expression was less marked in Sui68 and Sui72; expression was altogether absent in the remaining six cell lines. Expression of the *P16* product was noted in Sui67, Sui71 and Sui74, but the levels were quite low or absent in the other cell lines (Table 3).

Therapeutic studies with 5-FU. Using this panel of human pancreatic cancer-derived cell lines, we evaluated the effect of 5-FU in suppressing the proliferation of each cell line *in vitro*. Sui69 was excluded from the analysis, since its proliferation rate was quite slow. The other nine cell lines were subjected to the MTT assay and the results are shown in Fig. 2. Sui72 was about 10-fold more susceptible to the drug, whereas the other cell lines were resistant to the drug.

Based on this result, we conducted a study *in vivo*, in which the highly drug-susceptible Sui72 and the resistant Sui70 were implanted subcutaneously in SCID mice. The 5-FU levels tested were 50 and 100 mg/kg/head. As shown in Fig. 3, tumor formation was markedly suppressed in all the mice implanted with Sui72. This suppressive effect was dose dependent, suggesting the effectiveness of 5-FU against this cell line. On the other hand, 5-FU did not inhibit the formation of tumor following implantation of Sui70, reflecting the findings *in vitro*.

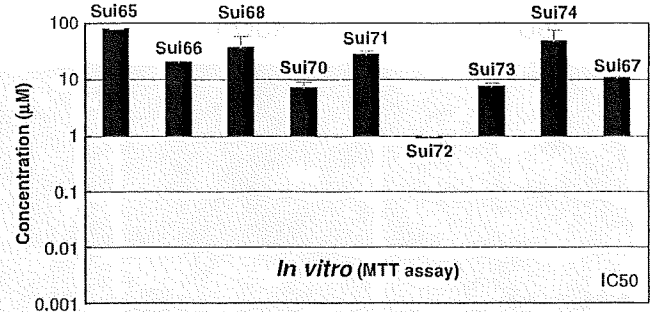

Fig. 2. Inhibition of growth of various human pancreatic cancer cell lines by 5-fluorouracil (5-FU) *in vitro*. The cell-growth inhibitory effects of 5-FU were assessed by the 3-(4,5-dimethylthiazol-2-yl)-2,5-diphenyltetrazolium bromide) (MTT) assay as described elsewhere.[21]

We attempted to identify the cause of the hypersensitivity of Sui72-5-FU by RT-PCR (Table 4). The mRNA expression levels of genes associated with the metabolisms of 5-FU, i.e. DHFR, EPGS, ECGF (TP), UPP1, PRPS1, TYMS (TS), UMPS (OPRT), TK1, MTHFR, NP (PNP) and UCK2 (UMPK) were analyzed in Sui72

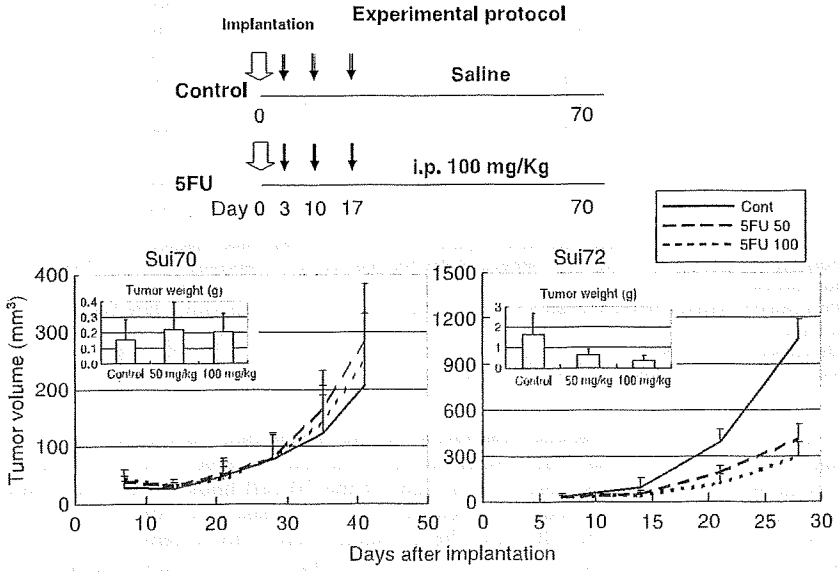

Fig. 3. Effect of 5-fluorouracil (5-FU) on Sui70 and Sui72 tumor growth in the SCID mouse. Six mice from each group were sacrificed when moribund, or on Day 28 or 40. The tumor mass was measured at predetermined time intervals in two dimensions with calipers, and the tumor volume was calculated according to the equation ($l \times w^2$)/2 [l = length, w = width].[18] Pancreatic carcinoma was confirmed by histopathology.

doi: 10.1111/j.1349-7006.2008.00896.x

Table 4. mRNA expression levels of genes related with 5-FU metabolism in a high sensitive Sui72 cells and in other human pancreatic cancer cell lines

Genes	Expression† The others‡	Expression† Sui72	Fold
DHFR	32.7 ± 37.8	33.1	1.0
FPGS	10.3 ± 18.3	n.d.	n.d.
TP	3.1 ± 4.6	0.1	0.0
UPP1	3.8 ± 5.0	1.6	0.4
PRPS1	9.1 ± 5.2	3.9	0.4
DPYD	0.6 ± 0.5	0.1	0.1
TYMS(TS)	49.9 ± 33.7	35.6	0.7
UMPS(OPRT)	7.2 ± 4.3	6.2	0.8
TK1	46.6 ± 46.3	28.4	0.6
MTHFR	4.4 ± 7.8	9.6	2.2
NP(PNP)	15.7 ± 8.0	23.3	1.5
UCK2(UMPK)	15.8 ± 9.7	29.7	1.9

n.d.: Not detectable by reverse transcription–polymerase chain reaction.
†Ratio of target gene/GAPD × 10-3 (fold).
‡The average ± SD of other cell lines except for Sui72.

as compared with other cell lines. Remarked decreased expression of DPYD was observed in Sui72 compared with other cell lines (0.6;/–0.5). These results suggest that lower expression of DPYD is the molecular determinant of high sensitivity to 5-FU in Sui72 cells.

Discussion

A number of cultured cell lines have been established from human pancreatic cancers[8–14] and have contributed greatly to advancing cancer research by allowing biological characterization (analysis of the features of proliferation, progression, etc.) of this cancer and being useful as a preclinical research tool in the evaluation of anticancer agents.[15,16] However, after multiple passages, some of these cell lines lose their initial properties (e.g. the histopathological features of the tumors formed following their implantation). There seems to be a universal necessity for enriching the research resources through establishment of new cancer cell lines which would reliably reflect the clinical features of this cancer. Pancreatic cancer is usually characterized by stromal cell infiltration, therefore it is relatively difficult to establish pancreatic cancer cell lines.[16] Bearing this in mind, we first attempted to establish pancreatic cell lines from the tumors formed in SCID mice following implantation of primary or metastatic pancreatic cancer tissue. In this way, we established 10 cell lines of the Sui series. Half of the 10 cell lines were positive for the tumor marker CA19-9, while all were positive for TPA. The histopathological profile of most of the 10 cell lines resembled that of the original tumor. These findings indicate that the cell lines of this Sui series are pancreatic cancer cell lines reliably reflecting the clinical features of pancreatic cancer. However, one of these cell lines (Sui69) did not form a tumor in the SCID mice, even though it was transplantable. This Sui69 cell line exhibited very slow proliferative activity. We are currently studying this cell line in NOD-SCID or NOG mice.

Pancreatic cancer cells often exhibit genetic alternations. Point mutation of the oncogene *K-ras*, loss of heterozygosity (LOH; 9p, 17p, 18q, 1q, etc.), point mutation of tumor suppresser genes at these chromosomal locations (*p16, p53, DPC4/AMAD4*, etc.), methylation of the promoter region, etc., have been reported in pancreatic cancer.[22–25] Of the 10 cell lines established in this study, *K-ras* point mutation[26,27] and *p53* mutation[28] were noted in eight cell lines, and the genetic alterations found resembled those seen in the clinical materials. In Sui73, both *K-ras* and *p53* were wild type. The *SMAD4/DPC4* gene is known to show a high frequency of alterations (50%), including mutation (20%) and deletion (30%).[29,30] Marked expression of the *SMDA4/DPC4* gene was observed in two cell lines, and less marked expression in two cell lines; expression was altogether absent in the remaining six cell lines. Analysis of expression of the *P16/CDKN2A/INK4A* product in the 10 established cell lines revealed its expression in three cell lines, but the expression was quite low or altogether absent in remaining seven cell lines. It has been suggested that in pancreatic cancer free of *P16* mutations or deletions, expression of this gene is absent because of abnormal methylation of the gene expression–adjusting region and that most pancreatic cancers show malfunctioning of *P16*.[30,31] These changes are seen commonly in many cases of pancreatic cancer and seem to determine the proliferative potential and tumorigenicity of pancreatic cancer cells.

When treating pancreatic cancer, surgical resection, one or a various combination of surgical resection, systemic chemotherapy and radiotherapy is selected depending on the stage of the cancer.[2,25,32] Conventionally, various regimens of adjuvant chemotherapy, primarily involving 5-FU, have been attempted,[3–5] but no valid means of treating pancreatic cancer have yet been established. We attempted to evaluate the efficacy of 5-FU (a drug used as a standard therapy for this cancer in the past) against the cell lines established by us in this study. When tested *in vitro*, Sui72 was susceptible to the drug, whereas the remaining eight lines (Sui70, etc.) were found to be resistant to the drug. This finding was endorsed by the results of the *in vivo* study. We then explored the molecular determinant of sensitivity of the Sui72 cell line to 5-FU. The results of the analysis suggest that the decreased expression of DPYD may be involved in the mechanism of cellular sensitivity to 5-FU. In addition, decreased expression of TYMS was also observed in Sui72 as compared with other cell lines. This observation might be consistent with high sensitivity to 5-FU of Sui72 cells.

Throughout this study, it was shown that the new cell lines of the Sui series are useful for research on pancreatic cancer (e.g. evaluation of pancreatic cancer cell proliferation and progression, evaluation of the efficacy of anticancer agents, and so on).

New anticancer agents (e.g. TS-1, which reinforces the efficacy of 5-FU),[33–35] and gemcitabine hydrochloride (GEM) have recently become available for clinical use,[36–38] with the expectation of extending the survival period of patients with pancreatic cancer. To date, however, no chemotherapeutic agents more efficacious than GEM for pancreatic cancer have been developed. Clinical studies have therefore been carried out, focusing on developing treatment regimens containing GEM in combination with some other drugs. If GEM were combined with TS-1 or other molecule-targeted drugs, further extension of the survival period of pancreatic cancer patients may be expected. In the near future, we propose to carry out preclinical studies to evaluate the efficacy of various anticancer agents in SCID mice implanted with the new cell lines derived from human pancreatic cancer and to identify the genes, etc. which determine the susceptibility of pancreatic cancer cells to anticancer agents. It also seems to be essential to develop a model of orthotopic implantation, with the goal of establishing a drug evaluation system more relevant to the clinical setting.[23]

In conclusion, we established 10 cell lines derived from human pancreatic cancers that were found to possess biological characteristics and genetic alterations unique to pancreatic cancer. These new cell lines are expected to be highly useful for analyzing the pattern of pancreatic cancer progression and evaluating the efficacy of anticancer agents.

Acknowledgments

This study was supported in part by a Grant-in-Aid for Cancer Research from the Ministry of Health, Labour and Welfare of Japan. We are grateful to M. Namae and R. Nakanishi for their excellent technical work.

References

1 Tsukuma H, Ajiki W, Ioka A, Oshima A. Survival of cancer patients diagnosed between 1993 and 1996: a collaborative study of population-based cancer registries in Japan. *Jpn J Clin Oncol* 2006; **36**: 602–7. Epub 2006 Jul 26.

2 Okusaka T, Matsumura Y, Aoki K. New approaches for pancreatic cancer in Japan. *Cancer Chemother Pharmacol* 2004; **54**: S78–82.

3 Ikeda M, Okada S, Ueno H *et al.* A phase II study of sequential methotrexate and 5-fluorouracil in metastatic pancreatic cancer. *Hepatogastroenterology* 2000; **47**: 862–5.

4 Ueno H, Okada S, Okusaka T, Ikeda M, Kuriyama H. Phase II study of uracil-tegafur in patients with metastatic pancreatic cancer. *Oncology* 2002; **62**: 223–7.

5 Okada S. Non surgical treatments of pancreatic cancer. *Int J Clin Oncol* 1999; **4**: 257–66.

6 Bhattacharyya M, Lemoine NR. Gene therapy developments for pancreatic cancer. *Best Pract Res Clin Gastroenterol* 2006; **20**: 285–98.

7 Lohr JM. Medical treatment of pancreatic cancer. *Expert Rev Anticancer Ther* 2007; **7**: 533–44.

8 Kato M, Shimada Y, Tanaka H *et al.* Characterization of six cell lines established from human pancreatic adenocarcinomas. *Cancer* 1999; **85**: 832–40.

9 Ku JL, Yoon KA, Kim WH *et al.* Establishment and characterization of four human pancreatic carcinoma cell lines. Genetic alterations in the TGFBR2 gene but not in the MADH4 gene. *Cell Tissue Res* 2002; **308**: 205–14. Epub 2002 Apr 11.

10 Kawano K, Iwamura T, Yamanari H, Seo Y, Suganuma T, Chijiiwa K. Establishment and characterization of a novel human pancreatic cancer cell line (SUIT-4) metastasizing to lymph nodes and lungs in nude mice. *Oncology* 2004; **66**: 458–67.

11 Starr AN, Vexler A, Marmor S *et al.* Establishment and characterization of a pancreatic carcinoma cell line derived from malignant pleural effusion. *Oncology* 2005; **69**: 239–45. Epub 2005 Sept 2.

12 Sato N, Mizumoto K, Beppu K *et al.* Establishment of a new human pancreatic cancer cell line, NOR-P1, with high angiogenic activity and metastatic potential. *Cancer Lett* 2000; **155**: 153–61.

13 Mohammad RM, Li Y, Mohamed AN *et al.* Clonal preservation of human pancreatic cell line derived from primary pancreatic adenocarcinoma. *Pancreas* 1999; **19**: 353–61.

14 Kimura Y, Kobari M, Yusa T *et al.* Establishment of an experimental liver metastasis model by intraportal injection of a newly derived human pancreatic cancer cell line (KLM-1). *Int J Pancreatol* 1996; **20**: 43–50.

15 Ulrich AB, Schmied BM, Standop J, Schneider MB, Pour PM. Pancreatic cell lines: a review. *Pancreas* 2002; **24**: 111–20.

16 Iwamura T, Hollingsworth MA. Pancreatic tumors. In: Master JRW, Palsson B, eds. *Human Cell Culture*. Great Britain: Kluwer Academic Publishers, 1999; 107–22.

17 Yanagihara K, Tanaka H, Takigahira M *et al.* Establishment of two cell lines from human gastric scirrhous carcinoma that possess the potential to metastasize spontaneously in nude mice. *Cancer Sci* 2004; **95**: 575–82.

18 Yanagihara K, Takigahira M, Tanaka H *et al.* Development and biological analysis of peritoneal metastasis mouse models for human scirrhous stomach cancer. *Cancer Sci* 2005; **96**: 323–32.

19 Sun C, Yamato T, Furukawa T, Ohnishi Y, Kijima H, Horii A. Characterization of the mutations of the K-ras, p53, p16, and SMAD4 genes in 15 human pancreatic cancer cell lines. *Oncol Rep* 2001; **8**: 89–92.

20 Yanagihara K, Seyama T, Tsumuraya M, Kamada N, Yokoro K. Establishment and characterization of human signet ring cell gastric carcinoma cell lines with amplification of the c-myc oncogene. *Cancer Res* 1991; **51**: 381–6.

21 Arao T, Yanagihara K, Takigahira M *et al.* ZD6474 inhibits tumor growth and intraperitoneal dissemination in a highly metastatic orthotopic gastric cancer model. *Int J Cancer* 2006; **118**: 483–9.

22 Rozenblum E, Schutte M, Goggins M *et al.* Tumor-suppressive pathways in pancreatic carcinoma. *Cancer Res* 1997; **57**: 1731–4.

23 Loukopoulos P, Kanetaka K, Takamura M, Shibata T, Sakamoto M, Hirohashi S. Orthotopic transplantation models of pancreatic adenocarcinoma derived from cell lines and primary tumors and displaying varying metastatic activity. *Pancreas* 2004; **29**: 193–203.

24 Yatsuoka T, Sunamura M, Furukawa T *et al.* Association of poor prognosis with loss of 12q, 17p, and 18q, and concordant loss of 6q/17p and 12q/18q in human pancreatic ductal adenocarcinoma. *Am J Gastroenterol* 2000; **95**: 2080–5.

25 Giovannetti E, Mey V, Nannizzi S, Pasqualetti G, Del Tacca M, Danesi R. Pharmacogenetics of anticancer drug sensitivity in pancreatic cancer. *Mol Cancer Ther* 2006; **5**: 1387–95.

26 Almoguera C, Shibata D, Forrester K, Martin J, Arnheim N, Perucho M. Most human carcinomas of the exocrine pancreas contain mutant c-K-ras genes. *Cell* 1988; **53**: 549–54.

27 Hruban RH, van Mansfeld AD, Offerhaus GJ *et al.* K-ras oncogene activation in adenocarcinoma of the human pancreas. A study of 82 carcinomas using a combination of mutant-enriched polymerase chain reaction analysis and allele-specific oligonucleotide hybridization. *Am J Pathol* 1993; **143**: 545–54.

28 Redston MS, Caldas C, Seymour AB *et al.* p53 mutations in pancreatic carcinoma and evidence of common involvement of homocopolymer tracts in DNA microdeletions. *Cancer Res* 1994; **54**: 3025–33.

29 Hahn SA, Schutte M, Hoque AT *et al.* DPC4, a candidate tumor suppressor gene at human chromosome 18q21.1. *Science* 1996; **271**: 350–3.

30 Wilentz RE, Su GH, Dai JL *et al.* Immunohistochemical labeling for dpc4 mirrors genetic status in pancreatic adenocarcinomas: a new marker of DPC4 inactivation. *Am J Pathol* 2000; **156**: 37–43.

31 Caldas C, Hahn SA, da Costa LT *et al.* Frequent somatic mutations and homozygous deletions of the p16 (MTS1) gene in pancreatic adenocarcinoma. *Nat Genet* 1994; **8**: 27–32.

32 Hochster HS, Haller DG, de Gramont A *et al.* Consensus report of the international society of gastrointestinal oncology on therapeutic progress in advanced pancreatic cancer. *Cancer* 2006; **107**: 676–85.

33 Kaneko T, Goto S, Kato A *et al.* Efficacy of immuno-cell therapy in patients with advanced pancreatic cancer. *Anticancer Res* 2005; **25**: 3709–14.

34 Zhu AX, Clark JW, Ryan DP *et al.* Phase I and pharmacokinetic study of S-1 administered for 14 days in a 21-day cycle in patients with advanced upper gastrointestinal cancer. *Cancer Chemother Pharmacol* 2007; **59**: 285–93. Epub 2006 Jun 20.

35 Sakata Y, Ohtsu A, Horikoshi N, Sugimachi K, Mitachi Y, Taguchi T. Late phase II study of novel oral fluoropyrimidine anticancer drug S-1 (1 M tegafur-0.4 M gimestat-1 M otastat potassium) in advanced gastric cancer patients. *Eur J Cancer* 1998; **34**: 1715–20.

36 Rothenberg ML, Moore MJ, Cripps MC *et al.* A phase II trial of gemcitabine in patients with 5-FU-refractory pancreas cancer. *Ann Oncol* 1996; **7**: 347–53.

37 Burris HA, 3rd Moore MJ, Andersen J *et al.* Improvements in survival and clinical benefit with gemcitabine as first-line therapy for patients with advanced pancreas cancer: a randomized trial. *J Clin Oncol* 1997; **15**: 2403–13.

38 Aristu J, Canon R, Pardo F *et al.* Surgical resection after preoperative chemoradiotherapy benefits selected patients with unresectable pancreatic cancer. *Am J Clin Oncol* 2003; **26**: 30–6.

doi: 10.1111/j.1349-7006.2008.00896.x

N-Glycan fucosylation of epidermal growth factor receptor modulates receptor activity and sensitivity to epidermal growth factor receptor tyrosine kinase inhibitor

Kazuko Matsumoto,[1,3] Hideyuki Yokote,[1] Tokuzo Arao,[1] Mari Maegawa,[1] Kaoru Tanaka,[1] Yoshihiko Fujita,[1] Chikako Shimizu,[2] Toshiaki Hanafusa,[3] Yasuhiro Fujiwara[2] and Kazuto Nishio[1,4]

[1]Department of Genome Biology, Kinki University School of Medicine, 377-2 Ohno-Higashi, Osaka-Sayama, Osaka; [2]Medical Oncology, National Cancer Center Hospital, Tokyo; [3]First Department of Internal Medicine, Osaka Medical College, Osaka, Japan

(Received January 15, 2008/Revised April 16, 2008/Accepted April 16, 2008/Online publication July 29, 2008)

The glycosylation of cell surface proteins is important for cancer biology processes such as cellular proliferation or metastasis. α1,6-Fucosyltransferase (FUT8) transfers a fucose residue to *n*-linked oligosaccharides on glycoproteins. Herein, we study the effect of fucosylation on epidermal growth factor receptor (EGFR) activity and sensitivity to an EGFR-specific tyrosine kinase inhibitor (EGFR-TKI). The increased fucosylation of EGFR significantly promoted EGF-mediated cellular growth, and the decreased fucosylation by stable FUT8 knockdown weakened the growth response in HEK293 cells. The overexpression of FUT8 cells were more sensitive than the control cells to the EGFR-TKI gefitinib, and FUT8 knockdown decreased the sensitivity to gefitinib. Finally, to examine the effects in a human cancer cell line, we constructed stable FUT8 knockdown A549 cells, and found that these cells also decreased EGF-mediated cellular growth and were less sensitive than the control cells to gefitinib. In conclusion, we demonstrated that the modification of EGFR fucosylation affected EGF-mediated cellular growth and sensitivity to gefitinib. Our results provide a novel insight into how the glycosylation status of a receptor may affect the sensitivity of the cell to molecular target agents. (*Cancer Sci* 2008; 99: 1611–1617)

The glycosylation of cell surface proteins and lipids is modified during the course of differentiation, growth and aging, and various glycoprotein structures are important for biological functions.[1] Proteins and lipids are modified with *n*-linked oligosaccharides in the endoplasmic reticulum and Golgi apparatus. *n*-Linked oligosaccharides contribute to the folding and stability of glycoproteins.[2] Various glycosyltransferases have been cloned and are known to be involved in the formation of *n*-linked oligosaccharides.[3,4] Accumulating data has demonstrated that the modification of glycoforms can even change the phenotype of cells.[5]

Regarding the relationship between malignancy and *n*-linked oligosaccharides, glycoproteins on the cell surface are known to be altered in both quantity and quality during cancerous transformation.[6] Genes are known to determine the specific structures of oligosaccharides during regulated biological processes involved in cancer, such as metastasis.[7] For example, the knockout of *n*-acetylglucosaminyltransferaseV (GnT-V) has been reported to decrease metastasis in mice, indicating that GnT-V is deeply involved in cancer metastasis.[8]

Epidermal growth factor receptor (EGFR) is frequently expressed or highly expressed in lung cancer, ovarian cancer and many other solid tumors,[9–12] and a high expression level in tumor cells is closely related to a poor prognosis.[13,14] Therefore, EGFR is considered an important therapeutic target for the treatment of solid tumors. Tyrosine kinase inhibitors (TKI) that target EGFR, like gefitinib (IRESSA, ZD1839)[15–17] and erlotinib (Tarceva),[18] and the anti-EGFR antibody cetuximab (IMC-C225),[19] have been reported to exhibit potential antitumor effects in some solid tumors. Dramatic responses to gefitinib have been observed in non-small cell lung cancer (NSCLC) patients harboring activating mutations in the *EGFR* gene involving an exon 19 deletion or an L858R point mutation in exon 21.[20,21] However, the sensitivity of a cell to EGFR-TKI cannot be completely defined by these mutations because tumor response and disease stabilization with gefitinib have also been reported in some NSCLC patients with wild-type EGFR.[22,23] We have searched for predictive biomarkers that determine sensitivity to molecular targeted agents, including gefitinib.[24,25] Of additional interest, EGFR contains 11 potential *n*-glycosylation sites in its extracellular domain.[26] α1,6-Fucosyltransferase (FUT8) catalyzes the transfer of a fucose group to the innermost *n*-acetylglucosamine residue of complex *n*-glycans via α1,6-linkage in mammals. Wang *et al.* clearly demonstrated that the fucosylation of EGFR catalyzed by FUT8 regulates its receptor activity and signaling in murine cells.[27] However, whether receptor fucosylation affects the sensitivity of human cells to molecular target agents remains uncertain.

Accordingly, we studied the relationship between the fucosylation status of EGFR and sensitivity to gefitinib in HEK293 and a human NSCLC cell, A549.

Materials and Methods

Reagents. Gefitinib (IRESSA, ZD1839) was provided by AstraZeneca (Cheshire, UK).

Expression constructs and viral production. A full-length cDNA of FUT8, originating from a NSCLC cell line (A549),[28] was amplified using a reverse transcriptase polymerase chain reaction (RT-PCR). A High Fidelity RNA PCR Kit (TaKaRa, Otsu, Japan) was used for the RT-PCR, and the following primer set was synthesized: forward, GGA AGT GAG TTG AAA ATC TGA AA; reverse, ACT GAG TTT GGT CGT TTA TCT CT. The PCR products were amplified again using Pyrobest DNA polymerase (TaKaRa) and the following primer set: forward, GCG CTA GCA ATG CGG CCA TGG ACT GGT TC; reverse, CGT GGT ACC TTT CTC AGC CTC AGG ATA TGT. After confirming the sequence, FUT8 cDNA was transferred to

[4]To whom correspondence should be addressed. E-mail: knishio@med.kindai.ac.jp

doi: 10.1111/j.1349-7006.2008.00847.x

pcDNA3.1 (Invitrogen, Carlsbad, CA, USA) with a FLAG-tag at its C-terminus. *EGFR* cDNA with a myc-tag in pcDNA3.1 and FUT8 cDNA with a FLAG-tag were cut out and transferred into a pQCLIN retroviral vector (BD Biosciences Clontech, San Diego, CA, USA) together with enhanced green fluorescent protein (EGFP) followed by the internal ribosome entry site sequence (IRES) to monitor the expression of the inserts indirectly. A pVSV-G vector (Clontech, Palo Alt, CA, USA) for the constitution of the viral envelope, pGP vector (TAKARA Bio) and the pQCXIX constructs were co-transfected into the HEK293 cells using FuGene6 transfection reagent (Roche Diagnostics, Basel, Switzerland). Briefly, 80% confluent cells cultured in a 10-cm dish were transfected with 2 μg pVSV-G plus 6 μg pQCXIX vectors. Forty-eight hours after transfection, the culture medium was collected and the viral particles were concentrated by centrifugation at 15 000*g* for 3 h at 4°C. The viral pellet was then resuspended in fresh RPMI-1640 medium. The titer of the viral vector was calculated by counting the EGFP-positive cells that were infected by serial dilutions of a virus-containing medium and then determining the multiplicity of infection (MOI).

FUT8 knockdown by shRNA. We constructed a retroviral vector that stably expressed short hairpin RNA (shRNA) targeting human FUT8. The DNA sequences were designed as follows: forward, GAT CCG TCT CAG AAT TGG CGC TAT GCT GTG AAG CCA CAG ATG GGC ATA GCG CCA ATT CTG AGA CTT TTT TG; reverse, AAT TCA AAA AAG TCT CAG AAT TGG CGC TAT GCC CAT CTG TGG CTT CAC AGC ATA GCG CCA ATT CTG AGA CG. These oligonucleotides were annealed and inserted into an RNAi-Ready pSIREN-RetroQ-ZsGreen vector (Clontech). The viral particles were produced as described in the viral production section.

Cell culture and transfection. HEK293 (a human embryonic kidney cell line) was maintained in Dulbecco's modified Eagle's medium (DMEM) medium and A549 (an NSCLC cell line) was maintained in RPMI-1640 medium supplemented with 10% fetal bovine serum (FBS). HEK293/EGFR cells were transfected with retrovirus containing FUT8 gene or shRNA for FUT8 (shFUT8) or shRNA control construct and designed as 293/EGFR/FUT8, 293/EGFR/shFUT8 and 293/EGFR/control, respectively. A549 cells were transfected with either shFUT8 or shRNA control and designed as A549/shFUT8 and A549/control, respectively.

α1,6-Fucosyltransferase activity assay. Cells were lysed with a lysis buffer containing 1% Triton X, 20 mM Tris-HCl (pH 8.0) and 50 mM NaCl. The fluorescent substrate (GnGn-bi-Asn-PABA; Fig. 1a) was purchased from Peptide Institute (Osaka, Japan). The standard mixture for measuring FUT8 activity contained 50 μM substrate, 200 mM MES (pH 7.0), 1% Triton X, 500 μM GDP-Fucose and the cell lysate in a final volume of 50 μL. The reaction mixture was incubated at 37°C for 6 h, and the reaction was stopped by heating at 100°C for 1 min. The sample was then centrifuged at 15 000*g* for 10 min and the supernatant (10 μL) was used for analysis. The product was separated using high-performance liquid chromatography (HPLC) with a TSK-gel ODS-80TM column (4.6 mm × 150 mm). Elution was performed at 55°C with a 20 mM acetate buffer, pH 4.0, containing 0.1% butanol. The fluorescence of the column elute was detected using a fluorescence photometer (Hitachi Fluorescence Spectrophotometer 650–10LC). The excitation and emission wavelengths were observed at 320 and 400 nm, respectively.[29]

Immunoprecipitation and immunoblotting. A549 cells were lysed with a lysis buffer containing 1% Triton X, 20 mM Tris-HCl (pH 7.0), 5 mM ethylenediaminetetraacetic acid (EDTA), 50 mM NaCl, 10 mM Na pyrophosphate, 50 mM NaF, 1 mM Na orthovanadate, and a Complete Mini protease inhibitor mix (Roche Diagnostics). The cell lysate (1 mg) was immunoprecipitated by incubation with anti-EGFR antibody (Upstate Biotechnology, Lake Placid, NY, USA) overnight, followed by further incubation with protein-G agarose (Santa Cruz Biotechnology, Santa Cruz, CA, USA) for 1 h and washed with lysis buffer three times. Whole cell lysates and immunoprecipitated samples were separated using sodium dodecylsulfate polyacrylamide gel electrophoresis (SDS-PAGE) and blotted on a polyvinylidene fluoride (PVDF) membrane. The membranes were blocked with 3% bovine serum albumin (BSA) in Tris-buffered saline with 0.05% Tween-20 (TBST) and then probed with monoclonal anti-EGFR antibody (Upstate Biotechnology), monoclonal phospho-tyrosine antibody, p44/42 MAP kinase antibody or phospho-p44/42 MAP kinase antibody (Cell Signaling, Beverly, MA, USA), followed by incubation with a monoclonal or polyclonal HRP-conjugated secondary antibody (Cell Signaling). An enhanced chemiluminescence detection system (GE Healthcare, Buckinghamshire, UK) was then used for visualization. Images were visualized by LAS-3000 (Fujifilm, Tokyo, Japan) and the data were quantified by automated densitometry using Multigauge ver. 3.0 (Fujifilm).

Lectin blotting. Whole cell lysates and immunoprecipitated samples were separated using SDS-PAGE and blotted on a PVDF membrane. The membrane was blocked with 5% BSA in TBST for 1 h at room temperature. The membrane was probed with biotinylated aleuria aurantia lectin (AAL, Seikagaku, Tokyo, Japan) for 1 h at room temperature, washed, and treated using the Vectastain ABC kit (Vector Laboratories, Burlingame, CA, USA) as a second antibody.

Cell proliferation assay. To evaluate the growth response to EGF stimulation, we used the tetrazolium dye (3,4,5-dimethyl-2H-tetrazolium bromide, MTT) assay. The cells were seeded at a density of 0.5–1.5 × 10^3 cells/well in 96-well plates under a serum-reduced condition (HEK293 cells, 4% FBS; A549 cells, 2% FBS). Twenty-four hours later, the cells were stimulated with EGF (R&D Systems, Minneapolis, MN, USA) at 20 ng/mL. After 48–72 h of incubation at 37°C, the MTT solution was added to each well and the plates were incubated for 3 h at 37°C. After centrifuging the plates at 400*g* for 5 min, the medium was discarded from each well, and 200 μL of dimethylsulfoxide was added to each well. The optical density was measured at 570 nm. For the growth curve experiments, the cells were seeded at a density of 2 × 10^3 cells/well in 96-well plates in the presence of 10% FBS or under the serum-reduced condition in the presence of 20 ng/mL of EGF. Cell proliferation was estimated by measuring the absorbance at 570 nm at 24 h intervals up to 72 h.

Growth inhibitory assay. To evaluate the growth inhibition in the presence of various concentrations of gefitinib, we used the MTT assay. The cells were seeded at a density of 1.5 or 2 × 10^3 cells/well in 96-well plates in the presence of 10% FBS or under the serum-reduced condition in the presence of 20 ng/mL of EGF. Twenty-four hours later, gefitinib was added and the incubation was continued further for 72 h at 37°C. The assay was conducted in triplicate.

Soft agar assay for colony formation. To confirm the data obtained from the growth inhibitory assay, we performed colony assays of A549 cells. Five hundred cells in 0.35% agar in DMEM containing 10% FBS and each concentration of EGF or gefitinib were seeded onto 6-well plates on an underlayer of 0.5% agar containing DMEM. The plates were incubated at 37°C for 14 days, and then the colonies were stained by crystal violet and counted under a microscope. The colony assay was performed in triplicate.

Statistical analysis. All statistical calculations were performed using a Student's *t*-test by StatView ver. 5 software (SAS Institute, Cary, NC, USA). $P < 0.05$ was considered significant.

Result

Establishment of FUT8 overexpression and knockdown cells. To examine whether an increase or decrease in the fucosylation of

doi: 10.1111/j.1349-7006.2008.00847.x

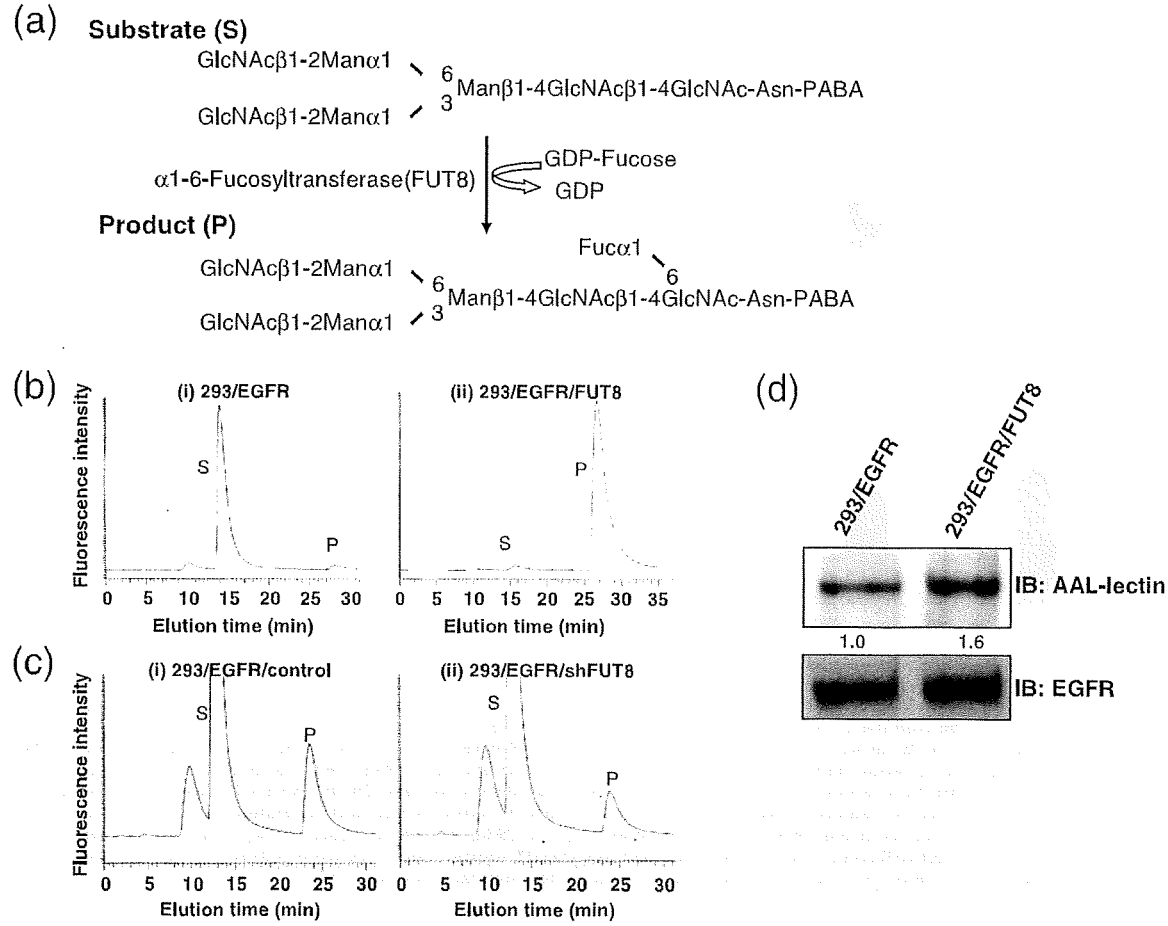

Fig. 1. α1,6-Fucosyltransferase (FUT8) enzyme activity of HEK293 cells. (a) Schema of FUT8 reaction pathway. Asn, asparagine; Fuc, Fucose; Man, mannose; PABA, 4-(2-pyridylamino) butylamine. (b) Analysis of FUT8 activity in cells overexpressing FUT8. FUT8 activity was measured using high-performance liquid chromatography. (i) 293/EGFR; (ii) 293/EGFR/FUT8. P, product; S, substrate. (c) Analysis of FUT8 activity in FUT8 knockdown cells. (i) 293/EGFR/control; (ii) 293/EGFR/shFUT8. (d) Effect of FUT8 overexpression on epidermal growth factor receptor (EGFR) fucosylation. The cell lysate from 293/EGFR or 293/EGFR/FUT8 cells was subjected to sodium dodecylsulfate polyacrylamide gel electrophoresis followed by lectin blotting using biotinylated *Aleuria aurantia* lectin (AAL). IB, immunoblot.

EGFR affected EGF-mediated cellular growth and sensitivity to gefitinib, we transfected EGFR and FUT8 retrovirally. We also constructed 293/EGFR/shFUT8 cells by the stable knockdown of intrinsic FUT8. FUT8 enzyme activity was measured by reverse-phase HPLC using a fluorescent substrate (GnGn-bi-Asn-PABA; Fig. 1a). FUT8 activity was 25-times higher in 293/EGFR/FUT8 cells than in 293/EGFR (44.1 U/L and 1.8 U/L, respectively; Fig. 1b). On the other hand, the activity in 293/EGFR/shFUT8 cells was 43% of that in 293/EGFR/control cells (Fig. 1c). We next compared fucosylated EGFR between 293/EGFR and 293/EGFR/FUT8 cells using lectin blotting with *Aleuria aurantia* lectin, which recognizes core fucosylation on *n*-glycans. The fucosylation of EGFR was increased in 293/EGFR/FUT8 cells, compared with that in 293/EGFR cells (Fig. 1d). These findings indicated that the overexpression or knockdown of FUT8 was functional and FUT8 regulated the fucosylation of EGFR, as expected.

EGFR fucosylation regulates EGF-mediated cellular growth in HEK293 and A549 cells. We next examined whether EGFR fucosylation affected the cellular growth in response to EGF ligand stimulation. Overexpression of FUT8 was associated with a significant increase, by approximately 20%, of the cellular growth in response to EGF stimulation ($P < 0.05$; Fig. 2a). In growth curve experiments, the proliferative activity of 293/EGFR/FUT8 cells was slightly increased as compared with that of 293/EGFR cells under normal conditions of culture in the presence of 10% FBS (Fig. 2b). The doubling times of 293/EGFR/FUT8 and 293/EGFR cells were 27.5 and 28.5 h, respectively. However, remarkable increase of the proliferative activity of 293/EGFR/FUT8 cells was observed as compared with that of the 293/EGFR cells in the presence of EGF stimulation ($P < 0.05$; Fig. 2c); the doubling times under this condition were 23.9 and 25.4 h, respectively. Next, FUT8 knockdown significantly decreased, by approximately 20%, the cellular growth in response to EGF stimulation ($P < 0.05$; Fig. 2d). In growth curve experiments, there was no difference in the proliferative activity between 293/EGFR/shFUT8 cells and 293/EGFR/control cells under normal conditions of culture (Fig. 2e), but significant decrease of the proliferative activity of 293/EGFR/shFUT8 cells was found as compared with that of the 293/EGFR/control cells in the presence of EGF stimulation ($P < 0.05$; Fig. 2f); the doubling times of the 293/EGFR/shFUT8 and 293/EGFR/control cells under this condition were 28.8 and 27.3 h, respectively. These findings suggest that the level of EGFR fucosylation regulated the cellular growth in response to EGF. To study whether the same phenomenon

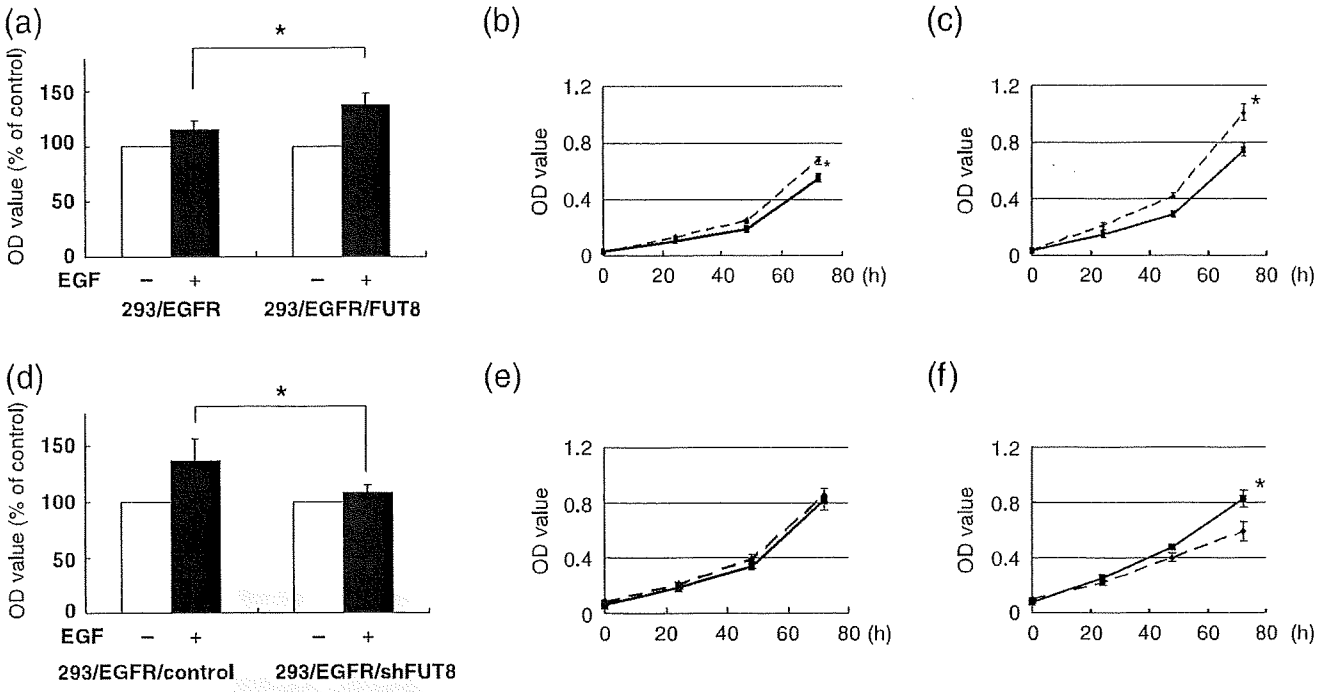

Fig. 2. Cellular growth response to epidermal growth factor (EGF) stimulation in HEK293 cells. (a) The 293/EGFR and 293/EGFR/FUT8 cells were seeded (1.5×10^3 cells/well) in 96-well plates under a serum-reduced condition and stimulated with 20 ng/mL of EGF and further incubated for 48 h at 37°C. (□), EGF (–); (■), EGF (+). (b) Growth curve experiments in the 293/EGFR (solid line) and 293/EGFR/FUT8 (dotted line) cells. The cells were cultured under a 10% fetal bovine serum (FBS) condition. (c) The 293/EGFR (solid line) and 293/EGFR/FUT8 (dotted line) cells were cultured under the presence of 20 ng/mL of EGF to a serum-reduced condition. (d) The 293/EGFR/control and 293/EGFR/shFUT8 cells were seeded (1.5×10^3 cells/well) in 96-well plates under a serum-reduced condition and stimulated with 20 ng/mL of EGF and incubated for 72 h at 37°C. (□), EGF (–); (■), EGF (+). (e) Growth curve experiments in the 293/EGFR/control (solid line) and 293/EGFR/shFUT8 (dotted line) cells. The cells were cultured under a 10% FBS condition. (f) The 293/EGFR/control (solid line) and 293/EGFR/shFUT8 (dotted line) cells were cultured under the presence of 20 ng/mL of EGF to a serum-reduced condition. OD value, 570 nm. *$P < 0.05$; scale lines, standard deviation (SD).

occurs in human cancer cells, we constructed A549/shFUT8, in which FUT8 was stably knocked down, and examined the relationship between the fucosylation level of EGFR and the response to EGF ligand stimulation. No FUT8 catalytic activity was detected by FUT8 knockdown in the A549 cells (Fig. 3a). A lectin blot analysis demonstrated that the fucosylation of EGFR was decreased in A549/shFUT8 cells, while the expression level of EGFR was similar in the control cells (Fig. 3b). We examined whether this reduction in EGFR fucosylation affected the EGF-mediated growth response. We found that A549/shFUT8 cells had significantly decreased EGF-mediated cellular growth by approximately 20%, compared with control cells ($P < 0.05$; Fig. 3c) by the MTT assay. In the growth curve experiments, a slight decrease of the proliferative activity of the A549/shFUT8 cells was observed as compared with that of the A549/control cells under normal conditions of culture in the presence of 10% FBS (Fig. 3d); the doubling times of the A549/shFUT8 and A549/control cells were 23.1 and 22.7 h, respectively. However, the A549/shFUT8 cells showed marked decrease of proliferative activity as compared with A549/control cells in the presence of EGF stimulation ($P < 0.05$, Fig. 3e); the doubling times of the A549/shFUT8 and A549/control cells were 22.2 and 20.8 h, respectively. These results suggest that the level of EGFR fucosylation regulated the cellular growth in response to EGF even in human cancer cells.

Modification of EGFR fucosylation affects cell sensitivity to gefitinib. We then examined whether an increase or decrease in EGFR fucosylation affected the sensitivity of HEK293 cells to gefitinib. Overexpression of FUT8 significantly enhanced the cellular sensitivity to gefitinib as compared with that of the control cells in the presence of EGF under a serum-reduced condition; the IC_{50} values of the drug for these cells were 3.5 ± 0.1 and 5.6 ± 0.3, respectively ($P < 0.05$; Fig. 4a). However, no significant difference in the IC_{50} values of the drug was noted between the two types of cells under normal culture conditions in the presence of 10% FBS (Fig. 4b). In addition, FUT8 knockdown significantly decreased the cellular sensitivity to gefitinib as compared with that of the control cells in the presence of EGF under the serum-reduced condition; the IC_{50} values of the drug for these cells were 7.3 ± 0.4 and 4.4 ± 1.0, respectively ($P < 0.05$; Fig. 4c). On the other hand, no significant difference in the IC_{50} values of the drug were noted among the cells when they were cultured under normal conditions (Fig. 4d). These results suggest that EGFR fucosylation modulates the cellular sensitivity to gefitinib.

We also examined the sensitivity of A549 cells to gefitinib. FUT8 knockdown significantly decreased the sensitivity of the A549 cells to gefitinib in the presence of 20 ng/mL of EGF under the serum-reduced condition; the IC_{50} values of the A549/shFUT8 and A549/control cells were 3.1 ± 0.3 and 1.3 ± 0.2, respectively ($P < 0.05$; Fig. 5a). However, no significant difference in the IC_{50} values were noted among the cells when they were cultured under normal conditions, similar to the observations for HEK293 cells (Fig. 5b). These results suggest that the EGFR fucosylation level affected the sensitivity of human cancer cells to gefitinib. To confirm the data obtained from the growth inhibitory assay, we performed colony assays with the A549 cells. Colony formation of A549/control, but not of the A549/shFUT8 cells, was significantly inhibited by 1 μM gefitinib ($P < 0.05$; Fig. 5c).

doi: 10.1111/j.1349-7006.2008.00847.x

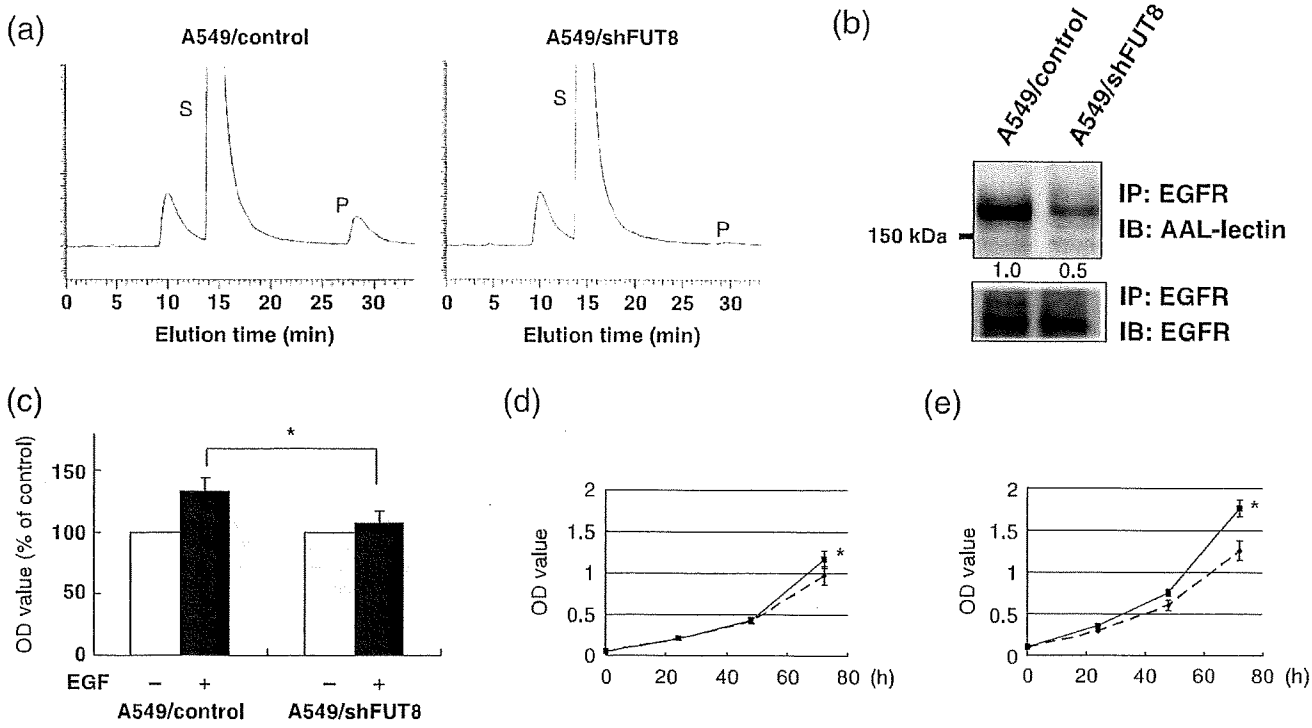

Fig. 3. α1,6-Fucosyltransferase (FUT8) knockdown weakened growth response to epidermal growth factor (EGF) stimulation in A549 cells. (a) FUT8 activity was analyzed using high-performance liquid chromatography. P, product; S, substrate. (b) Effect of FUT8 knockdown on EGF receptor (EGFR) fucosylation in A549 cells. The cell lysate was immunoprecipitated using anti-EGFR antibody, and the sample was separated using sodium dodecylsulfate polyacrylamide gel electrophoresis followed by blotting biotinylated *Aleuria aurantia* lectin (AAL) or monoclonal anti-EGFR antibody. IB, immunoblot; IP, immunoprecipitate. (c) The cells were seeded (0.5×10^3 cells/well) in 96-well plates under a serum-reduced condition. Twenty-four hours later, the cells were stimulated with 20 ng/mL of EGF and further incubated for 48 h. (□), EGF (–); (■), EGF (+). (d) Growth curve experiments in the A549/control (solid line) and A549/shFUT8 (dotted line) cells. The cells were cultured under a 10% fetal bovine serum condition. (e) The A549/control (solid line) and A549/shFUT8 (dotted line) cells were cultured under the presence of 20 ng/mL of EGF to a serum-reduced condition. OD value, 570 nm. $*P < 0.05$; scale lines, standard deviation.

Fucosylation status of EGFR regulates EGFR signaling. We examined the effect of FUT8 knockdown on the phosphorylation levels of EGFR and the EGFR-mediated intracellular signaling pathway in A549 cells. FUT8 knockdown decreased the phosphorylation levels of EGFR in the presence of EGF stimulation (Fig. 5d). FUT8 knockdown also decreased the EGF-mediated phosphorylation of mitogen-activated protein kinase in the presence of 0.2 and 2 ng/mL of EGF (Fig. 5e). These results suggest that low EGFR fucosylation levels decrease the EGFR-mediated intracellular signaling pathway's response to EGF stimulation.

Discussion

The purpose of this study was to investigate whether the modification of EGFR fucosylation affected EGF-mediated cellular growth and cell sensitivity to gefitinib. We found that the increase in EGFR fucosylation resulting from FUT8 overexpression enhanced the response to EGF stimulation and the sensitivity of the cells to gefitinib. A decrease in EGFR fucosylation resulting from FUT8 knockdown weakened the EGF-mediated cellular growth response and cell sensitivity.

Two possible mechanisms may explain how EGFR fucosylation affects the EGF-mediated growth response. First, the binding affinity of EGFR to the EGF ligand might be affected by the modified fucosylation of the receptor. *n*-Acetylglucosaminyltransferase III (GnT III) is known to catalyze the addition of *n*-acetylglucosamine in β1-4 linkage to the β-linked mannose of the trimannosyl core of *n*-linked oligosaccharides to produce a bisecting GlcNac residue. Rebbaa *et al.* reported that the overexpression of GnT III in glioma cells modifies the glycosylation of its receptor, resulting in a decrease in EGF binding and EGFR autophosphorylation;[30] this finding suggests that the carbohydrate structure at the extracellular domain of EGFR affects the binding affinity with its ligand and the receptor activity. This evidence supports this first possible mechanism. Another possibility is that the ability of the receptor to form dimers might be affected by the glycosylation of the receptor. Tsuda *et al.* reported that a specific *n*-glycosylation mutant of domain III of EGFR leads to ligand-independent dimerization and phosphorylation, resulting in the spontaneous activation of the receptor.[31] These findings indicate that *n*-linked oligosaccharides in extracellular domain III of EGFR play a crucial role in receptor dimerization, independent of ligand binding. The type III EGFR (EGFRvIII), which lacks exons 2–7 in the extracellular domain, is constitutively phosphorylated independently of EGF-ligand stimulation. Fernandes *et al.* demonstrated that the receptor–receptor self association is highly dependent on a conformation induced by *n*-linked glycosylation, suggesting that *n*-linked oligosaccharides play an important role in this autodimerization.[32]

Regarding fucosylation, Wang *et al.* reported that EGF decreased EGF binding to EGFR in Fut8 knockout mice, resulting in a higher responsiveness of the receptor to its ligand.[27] Many studies have reported that the *mutant* EGFR (i.e. 15-base deletion or L858R) signaling is constitutively active without ligand condition. Thus, we speculated that wild-type EGFR

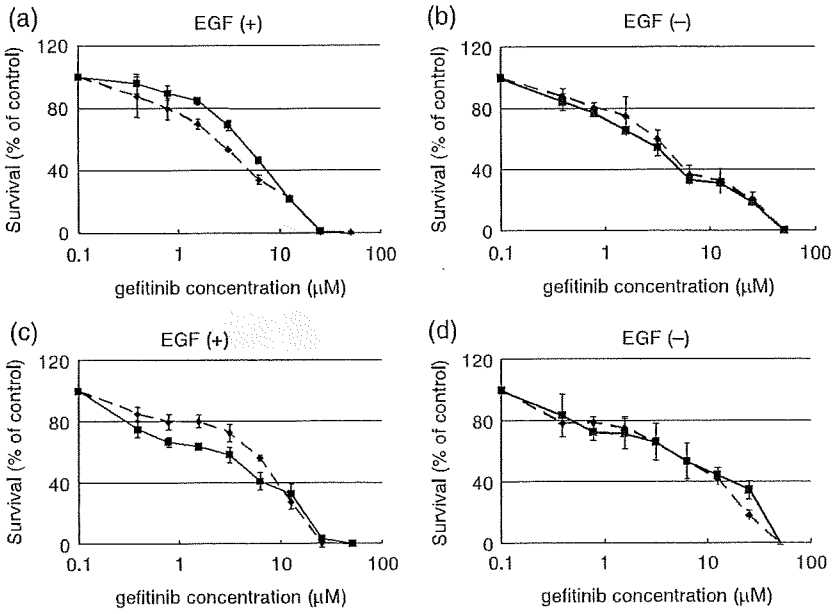

Fig. 4. Sensitivity of HEK293 cells to gefitinib. The cells were seeded at a density of 2×10^3 cells/well in 96-well plates. Twenty-four hours later, the cells were exposed to gefitinib and were then incubated for 72 h at 37°C. The cell growth was quantitated using an 3,4,5-dimethyl-2H-tetrazolium bromide (MTT) assay. (a) 293/EGFR (solid line) and 293/EGFR/FUT8 (dotted line) were cultured under the presence of 20 ng/mL of EGF to a serum-reduced condition. (b) 293/EGFR (solid line) and 293/EGFR/FUT8 (dotted line) were cultured under a 10% fetal bovine serum (FBS) condition. (c) 293/EGFR/control cells (solid line) and 293/EGFR/shFUT8 cells (dotted line) were cultured under the presence of 20 ng/mL of EGF to a serum-reduced condition. (d) 293/EGFR/control cells (solid line) and 293/EGFR/shFUT8 cells (dotted line) were cultured under a 10% FBS condition. Scale lines, standard deviation.

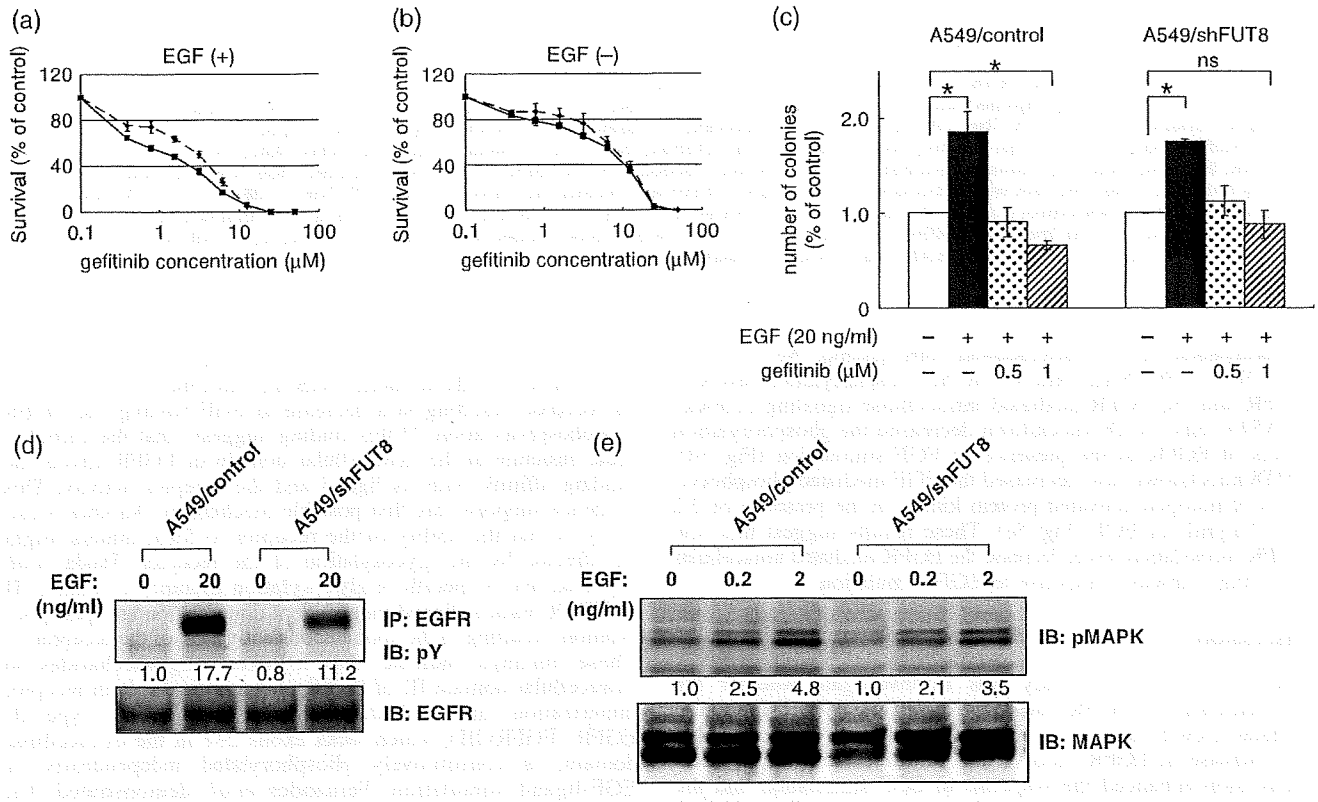

Fig. 5. α1,6-Fucosyltransferase (FUT8) knockdown decreased the sensitivity of A549 cells to gefitinib, epidermal growth factor receptor (EGFR) phosphorylation and EGFR-mediated intracellular signaling. (a) A549/control cells (solid line) and A549/shFUT8 cells (dotted line) were seeded at a density of 1.5×10^3 cells/well in 96-well plates. Twenty-four hours later, the cells were exposed to gefitinib and were then incubated for 72 h at 37°C. The cells were cultured under the presence of 20 ng/mL of EGF to a serum-reduced condition. (b) A549/control cells (solid line) and A549/shFUT8 cells (dotted line) were cultured under a 10% fetal bovine serum condition. Scale lines, standard deviation (SD). (c) Colony assay in A549/control cells and A549/shFUT8 cells. The cells were cultured for 14 days under the presence or absence of EGF or gefitinib. $*P < 0.05$; scale lines, SD. (d) A549 cells were cultured under a serum-free condition for 6 h, and the cells were stimulated with 20 ng/mL of EGF for 10 min. The cell lysate was immunoprecipitated using anti-EGFR antibody and immunoblotted using antiphospho-tyrosine antibody (pY). (e) A549 cells were stimulated with 0.2 ng/mL or 2 ng/mL EGF for 10 min. The cell lysate was separated using sodium dodecylsulfate polyacrylamide gel electrophoresis and then immunoblotted using antiphospho p44/42 mitogen-activated protein kinase (pMAPK) antibody and antip44/42 MAPK (MAPK) antibody. IB, immunoblot; IP, immunoprecipitate.

doi: 10.1111/j.1349-7006.2008.00847.x

might be suitable for a study of the effects of fucosylation. Our results also demonstrate that modifications of EGFR fucosylation through the overexpression or knockdown of FUT8 alter EGF-mediated cellular growth responses in both HEK293 and A549 cells.

Epidermal growth factor receptor is overexpressed in various human tumors, and the overexpression of EGFR is associated with a poor prognosis.[33] Many researchers have studied the biological and clinical significance of *EGFR* mutations, including exon 19 deletions and the L858R point mutation in exon 21, which behave like constitutively-active receptors.[34-36] Patients with constitutively-active mutants of *EGFR* are more sensitive to gefitinib. However, some patients respond to EGFR-TKI even though they do not carry such *EGFR* mutations;[22,23] suggesting the presence of one or more undefined factors that affects sensitivity to gefitinib in addition to *EGFR* mutations. Although the impact on sensitivity to gefitinib is smaller than that of EGFR mutations, we have shown that modifications in wild-type EGFR fucosylation also affect sensitivity to gefitinib. Our findings raise the possibility that the status of EGFR fucosylation may be another determinant of sensitivity to gefitinib.

In conclusion, we have demonstrated that the fucosylation level of EGFR, which was regulated by FUT8, modifies EGF-mediated cellular growth and affects sensitivity to gefitinib.

Acknowledgments

This work was supported by funds for the Third-Term Comprehensive 10-Year Strategy for Cancer Control and for Health and Labor Scientific Research Grants, Research on Advanced Medical Technology H17-Pharmaco-006. K. M is the recipient of a Research Resident Fellowship from the Foundation of Promotion of Cancer Research in Japan.

References

1 Hakomori Si SI. Inaugural Article: The glycosynapse. *Proc Natl Acad Sci USA* 2002; **99**: 225–32.
2 Helenius A, Aebi M. Intracellular functions of N-linked glycans. *Science* 2001; **291**: 2364–9.
3 Sato T, Furukawa K, Bakker H, Van den Eijnden DH, Van Die I. Molecular cloning of a human cDNA encoding beta-1,4-galactosyltransferase with 37% identity to mammalian UDP-Gal: GlcNAc beta-1,4-galactosyltransferase. *Proc Natl Acad Sci USA* 1998; **95**: 472–7.
4 Almeida R, Amado M, David L *et al.* A family of human beta4-galactosyltransferases. Cloning and expression of two novel UDP-galactose: beta-n-acetylglucosamine beta1, 4-galactosyltransferases, beta4Gal-T2 and beta4Gal-T3. *J Biol Chem* 1997; **272**: 31 979–91.
5 Coetzee T, Fujita N, Dupree J *et al.* Myelination in the absence of galactocerebroside and sulfatide: normal structure with abnormal function and regional instability. *Cell* 1996; **86**: 209–19.
6 Dennis JW. Asn-linked oligosaccharide processing and malignant potential. *Cancer Surv* 1988; **7**: 573–95.
7 Dennis JW, Laferte S, Waghorne C, Breitman ML, Kerbel RS. Beta 1-6 branching of Asn-linked oligosaccharides is directly associated with metastasis. *Science* 1987; **236**: 582–5.
8 Granovsky M, Fata J, Pawling J, Muller WJ, Khokha R, Dennis JW. Suppression of tumor growth and metastasis in Mgat5-deficient mice. *Nat Med* 2000; **6**: 306–12.
9 Ang KK, Berkey BA, Tu X *et al.* Impact of epidermal growth factor receptor expression on survival and pattern of relapse in patients with advanced head and neck carcinoma. *Cancer Res* 2002; **62**: 7350–6.
10 Rusch V, Klimstra D, Venkatraman E, Pisters PW, Langenfeld J, Dmitrovsky E. Overexpression of the epidermal growth factor receptor and its ligand transforming growth factor alpha is frequent in resectable non-small cell lung cancer but does not predict tumor progression. *Clin Cancer Res* 1997; **3**: 515–22.
11 Watanabe K, Tachibana O, Sata K, Yonekawa Y, Kleihues P, Ohgaki H. Overexpression of the EGF receptor and p53 mutations are mutually exclusive in the evolution of primary and secondary glioblastomas. *Brain Pathol* 1996; **6**: 217–23; discussion 23–4.
12 Lipponen P, Eskelinen M. Expression of epidermal growth factor receptor in bladder cancer as related to established prognostic factors, oncoprotein (c-erbB-2, p53) expression and long-term prognosis. *Br J Cancer* 1994; **69**: 1120–5.
13 Khorana AA, Ryan CK, Cox C, Eberly S, Sahasrabudhe DM. Vascular endothelial growth factor, CD68, and epidermal growth factor receptor expression and survival in patients with Stage II and Stage III colon carcinoma: a role for the host response in prognosis. *Cancer* 2003; **97**: 960–8.
14 Magne N, Pivot X, Bensadoun RJ *et al.* The relationship of epidermal growth factor receptor levels to the prognosis of unresectable pharyngeal cancer patients treated by chemo-radiotherapy. *Eur J Cancer* 2001; **37**: 2169–77.
15 Koizumi F, Kanzawa F, Ueda Y *et al.* Synergistic interaction between the EGFR tyrosine kinase inhibitor gefitinib ('Iressa') and the DNA topoisomerase I inhibitor CPT-11 (irinotecan) in human colorectal cancer cells. *Int J Cancer* 2004; **108**: 464–72.
16 Naruse I, Ohmori T, Ao Y *et al.* Antitumor activity of the selective epidermal growth factor receptor-tyrosine kinase inhibitor (EGFR-TKI) Iressa (ZD1839) in an EGFR-expressing multidrug-resistant cell line in vitro and in vivo. *Int J Cancer* 2002; **98**: 310–15.
17 Fukuoka M, Yano S, Giaccone G *et al.* Multi-institutional randomized phase II trial of gefitinib for previously treated patients with advanced non-small-cell lung cancer. *J Clin Oncol* 2003; **21**: 2237–46.
18 Sandler A. Clinical experience with the HER1/EGFR tyrosine kinase inhibitor erlotinib. *Oncology (Huntingt)* 2003; **17**: 17–22.
19 Herbst RS, Hong WK. IMC-C225, an anti-epidermal growth factor receptor monoclonal antibody for treatment of head and neck cancer. *Semin Oncol* 2002; **29**: 18–30.
20 Lynch TJ, Bell DW, Sordella R *et al.* Activating mutations in the epidermal growth factor receptor underlying responsiveness of non-small-cell lung cancer to gefitinib. *N Engl J Med* 2004; **350**: 2129–39.
21 Paez JG, Janne PA, Lee JC *et al.* EGFR mutations in lung cancer: correlation with clinical response to gefitinib therapy. *Science* 2004; **304**: 1497–500.
22 Han SW, Kim TY, Hwang PG *et al.* Predictive and prognostic impact of epidermal growth factor receptor mutation in non-small-cell lung cancer patients treated with gefitinib. *J Clin Oncol* 2005; **23**: 2493–501.
23 Takano T, Ohe Y, Sakamoto H *et al.* Epidermal growth factor receptor gene mutations and increased copy numbers predict gefitinib sensitivity in patients with recurrent non-small-cell lung cancer. *J Clin Oncol* 2005; **23**: 6829–37.
24 Kimura H, Kasahara K, Kawaishi M *et al.* Detection of epidermal growth factor receptor mutations in serum as a predictor of the response to gefitinib in patients with non-small-cell lung cancer. *Clin Cancer Res* 2006; **12**: 3915–21.
25 Sakai K, Yokote H, Murakami-Murofushi K, Tamura T, Saijo N, Nishio K. In-frame deletion in the EGF receptor alters kinase inhibition by gefitinib. *Biochem J* 2006; **397**: 537–43.
26 Whitson KB, Whitson SR, Red-Brewer ML *et al.* Functional effects of glycosylation at Asn-579 of the epidermal growth factor receptor. *Biochemistry* 2005; **44**: 14 920–31.
27 Wang X, Gu J, Ihara H, Miyoshi E, Honke K, Taniguchi N. Core fucosylation regulates epidermal growth factor receptor-mediated intracellular signaling. *J Biol Chem* 2006; **281**: 2572–7.
28 Fukuoka K, Nishio K, Fukumoto H *et al.* Ectopic p16 (ink4) expression enhances CPT-11-induced apoptosis through increased delay in S-phase progression in human non-small-cell-lung-cancer cells. *Int J Cancer* 2000; **86**: 197–203.
29 Uozumi N, Teshima T, Yamamoto T *et al.* A fluorescent assay method for GDP-L-Fuc: N-acetyl-beta-D-glucosaminide alpha 1-6fucosyltransferase activity, involving high performance liquid chromatography. *J Biochem (Tokyo)* 1996; **120**: 385–92.
30 Rebbaa A, Yamamoto H, Saito T *et al.* Gene transfection-mediated overexpression of beta1,4-N-acetylglucosamine bisecting oligosaccharides in glioma cell line U373 MG inhibits epidermal growth factor receptor function. *J Biol Chem* 1997; **272**: 9275–9.
31 Tsuda T, Ikeda Y, Taniguchi N. The Asn-420-linked sugar chain in human epidermal growth factor receptor suppresses ligand-independent spontaneous oligomerization. Possible role of a specific sugar chain in controllable receptor activation. *J Biol Chem* 2000; **275**: 21 988–94.
32 Fernandes H, Cohen S, Bishayee S. Glycosylation-induced conformational modification positively regulates receptor–receptor association: a study with an aberrant epidermal growth factor receptor (EGFRvIII/DeltaEGFR) expressed in cancer cells. *J Biol Chem* 2001; **276**: 5375–83.
33 Selvaggi G, Novello S, Torri V *et al.* Epidermal growth factor receptor overexpression correlates with a poor prognosis in completely resected non-small-cell lung cancer. *Ann Oncol* 2004; **15**: 28–32.
34 Tracy S, Mukohara T, Hansen M, Meyerson M, Johnson BE, Janne PA. Gefitinib induces apoptosis in the EGFRL858R non-small-cell lung cancer cell line H3255. *Cancer Res* 2004; **64**: 7241–4.
35 Chen YR, Fu YN, Lin CH *et al.* Distinctive activation patterns in constitutively active and gefitinib-sensitive EGFR mutants. *Oncogene* 2006; **25**: 1205–15.
36 Sordella R, Bell DW, Haber DA, Settleman J. Gefitinib-sensitizing EGFR mutations in lung cancer activate anti-apoptotic pathways. *Science* 2004; **305**: 1163–7.

Pertuzumab, a novel HER dimerization inhibitor, inhibits the growth of human lung cancer cells mediated by the HER3 signaling pathway

Kazuko Sakai,[1,3] Hideyuki Yokote,[1,4] Kimiko Murakami-Murofushi,[3] Tomohide Tamura,[2] Nagahiro Saijo[2] and Kazuto Nishio[1,4,5]

[1]Shien-Laboratory,[2]Medical Oncology, National Cancer Center Hospital; Tsukiji 5-1-1, Chuo-ku, Tokyo 104-0045; [3]Department of Biology, Faculty of Science, Ochanomizu University, Ohtsuka 2-1-1, Bunkyo-ku, Tokyo 112-8610; [4]Depatment of Genome Biology, Kinki University School of Medicine, 377-2 Ohno-Higashi, Osaka-Sayama, Osaka 589-8511, Japan

(Received December 18, 2006/Revised April 4, 2007/Accepted May 10, 2007/Online publication July 9, 2007)

A humanized anti-HER2 monoclonal antibody pertuzumab (Omnitarg, 2C4), binding to a different HER2 epitope than trastuzumab, is known as an inhibitor of heterodimerization of the HER receptors. Potent antitumor activity against HER2-expressing breast and prostate cancer cell lines has been clarified, but this potential is not clear against lung cancers. The authors investigated the *in vitro* anti-tumor activity of pertuzumab against eight non-small cell lung cancer cells expressing various members of the HER receptors. A lung cancer 11_18 cell line expressed a large amount of HER2 and HER3, and its cell growth was stimulated by an HER3 ligand, heregulin (HRG)-α. Pertuzumab significantly inhibited the HRG-α-stimulated cellular growth of the 11_18 cells. Pertuzumab blocked HRG-α-stimulated phosphorylation of HER3, mitogen-activated protein kinase (MAPK), and Akt. In contrast, pertuzumab failed to block epidermal growth factor (EGF)-stimulated phosphorylation of EGF receptor (EGFR) and MAPK. Immunoprecipitation showed that pertuzumab inhibited HRG-α-stimulated HER2/HER3 heterodimer formation. HRG-α-stimulated HER3 phosphorylation was also observed in the PC-9 cells co-overexpressing EGFR, HER2, and HER3, but the cell growth was neither stimulated by HRG-α nor inhibited by pertuzumab. The present results suggest that pertuzumab is effective against HRG-α-dependent cell growth in lung cancer cells through inhibition of HRG-α-stimulated HER2/HER3 signaling. (*Cancer Sci* 2007; 98: 1498–1503)

The HER family of receptor tyrosine kinases consists of four members: EGFR (also termed HER1/ErbB-1), HER2/ErbB-2/Neu, HER3/ErbB-3, and HER4/ErbB-4.[1] Binding of ligands leads to the homo- and heterodimer formation of the receptor tyrosine kinase.[2] There are numerous HER-specific ligands that generate signaling diversity within the cell.[3] EGF, amphiregulin, and TGF-α are known as a specific ligand of EGFR. HB-EGF, β-cellulin, and epiregulin have dual specificity for binding to EGFR and HER4. HRG-α binds HER3 and HER4.[4] No direct ligand for HER2 has been discovered. Dimerization consequently stimulates the intrinsic tyrosine kinase activity of receptors, and activates the downstream-signaling molecules such as MAPK, Akt, JAK, and STAT.[5,6]

Pertuzumab is a humanized monoclonal antibody and binds to the dimerization domain of HER2 distinct from the domain that trastuzumab binds to.[7] Therefore, pertuzumab is known as a dimerization inhibiter between HER2 and the other HER family receptors. A phase I trial of pertuzumab has been performed for advanced tumors,[8] and phase II studies of pertuzumab are underway. Two members of the HER family, HER2 and HER3, act as key oncogenes in breast cancer cells.[9,10] *In vitro* and *in vivo* anti-tumor activities of pertuzumab have been reported in breast tumors through the inhibition of the HER2/HER3 heterodimer formation.[11,12] In lung cancer cells, EGFR plays a crucial role in their biological behavior, but it is unclear whether pertuzumab inhibits the growth of the lung cancer cells mediated by HER family receptors.

The authors have focused on the growth inhibitory effect of pertuzumab against NSCLC cells expressing different types of HER receptors, and analyzed the mechanism of action of pertuzumab in response to the HER receptor ligand.

Materials and Methods

Reagents. Pertuzumab (Omnitarg, 2C4) was provided in sterile water at 25 mg/mL by Genentech, Inc. (South San Francisco, CA, USA) before use. All chemicals and reagents were purchased from Sigma (St Louis, MO, USA) unless noted otherwise.

Cell lines. The human NSCLC cell lines PC-7, PC-9, and PC-14 (Tokyo Medical University, Tokyo, Japan),[13,14] A549 (American Type Culture Collection, Manassas, VA, USA), and PC-3, Ma-1, Ma-24, and 11_18,[15] were maintained in RPMI 1640 medium supplemented with 10% heat-inactivated FBS (Life Technologies, Rockville, MD, USA).

Cell stimulation and lysis. Cells were starved in serum free RPMI 1640 medium for 24 h and treated with EGF, TGF-α, HB-EGF, and HRG-α at 100 ng/mL for 10 min. Cells were washed twice with ice-cold PBS, and lysed with lysis buffer (50 mM Tris, pH 7.5, 150 mM NaCl, 1% Nonidet P-40, 1 mM EDTA, 5 mM sodium pyrophosphate, 50 mM NaF, 1 mM sodium vanadate, 4 mg/mL leupeptin, 4 mg/mL apoprotein, 1 mM PMSF). Protein concentration of the supernatants was determined by the BCA protein assay (Pierce, Rockford, IL, USA).

Immunoprecipitation. Cell lysates (1000 μg) were incubated with the anti-HER2 antibody (Santa Cruz Biotechnology, Santa Cruz, CA, USA) at 4°C overnight. Protein G magnetic beads (New England BioLabs, Beverly, MA, USA) were added for 2 h. Beads were washed three times with lysis buffer, resuspended in SDS sample buffer with 2% β-mercaptoethanol, boiled, and separated using SDS-PAGE.

Western blotting. Cell lysates were electrophoretically separated on SDS-PAGE and transferred to a polyvinylidene difluoride

[5]To whom correspondence should be addressed. E-mail: knishio@med.kindai.ac.jp

Abbreviations: BCA, bicinchoninic acid; ECL, electrochemiluminescence; EDTA, ethylene diamine tetra-acetic acid; EGF, epidermal growth factor; EGFR, epidermal growth factor receptor; FBS, fetal bovine serum; HB-EGF, heparin-binding epidermal growth factor; HRG-α, heregulin-α; JAK, Janus kinase; MAPK, mitogen-activated protein kinase; MTS, 3-(4,5-dimethylthiazol-2-yl)-5-(3-carboxymethoxyphenyl)-2-(4-sulfophenyl)-2H-tetrazolium; NSCLC, non-small cell lung cancer; PBS, phosphate-buffered saline; PMSF, phenylmethylsulfonyl fluoride; RPMI, Roswell Park Memorial Institute; SDS-PAGE, sodium dodecyl sulfate-polyacrylamide gel electrophoresis; STAT, signal transducer and activator of transcription; TGF-α, transforming growth factor-α.

doi: 10.1111/j.1349-7006.2007.00553.x

membrane (Millipore, Bedford, MA, USA). The membrane was probed with each antibody against EGFR and HER2 (Transduction Laboratory, San Diego, CA, USA), HER3 (Santa Cruz Biotechnology), phospho-EGFR (Tyr1068), phospho-HER3 (Tyr1289), MAPK, phospho-MAPK (Thr202/204), Akt, phospho-Akt (Ser473) (Cell Signaling, Beverly, MA, USA), phosphotyrosine (PY-20, Transduction Laboratory), and β-actin (Sigma) as the first antibody, followed by detection using a horseradish peroxidase-conjugated secondary antibody. The bands were visualized with ECL (Amersham, Piscataway, NJ, USA), and images of blotted patterns were analyzed with NIH image software (National Institutes of Health, Bethesda, MD, USA).

Growth inhibition assay. A 100-μL volume of cell suspension (5000 cells/well) in serum-free RPMI 1640 medium was seeded into a 96-well plate and 50 μL of each drug at various concentrations and 50 μL of EGF, TGF-α, HB-EGF, and HRG-α, at 100 ng/mL was added. Human IgG1 (Calbiochem, Cambridge, MA, USA) was used as isotype control. After incubation for 72 h at 37°C, 20 μL of MTS solution (Promega, Madison, WI, USA) was added to each well and the plates were incubated for a further 2 h at 37°C. The absorbance readings for each well were determined at 490 nm with a Delta-soft on a Macintosh computer (Apple, Cupertino, CA, USA) interfaced to a Bio-Tek Microplate Reader EL-340 (BioMetallics, Princeton, NJ, USA). For ligand-stimulated growth of cells, the experiment was performed in six replicate wells for each ligand and carried out independently three times. For growth inhibition of pertuzumab, the experiment was performed in three replicate wells for each drug concentration and carried out independently three times as described elsewhere.[16]

Results

HRG-α dependent cell growth in lung cancer cells. Ligand-dependent cell growth of lung cancer cells was examined (Fig. 1). The addition of EGF, TGF-α, and HB-EGF increased the cell growth of the PC-3, 11_18, and A549 cells, but not that of the PC-7, PC-9, PC-14, Ma-1, and Ma-24 cells. HRG-α addition significantly increased the growth of the 11_18 cells (390% of control, $P < 0.01$ by t-test) and Ma-24 cells (204% of control, $P < 0.01$ by t-test), but did not influence the growth of any other cells. These findings suggest that the growth of the 11_18 and Ma-24 cells is depending upon HRG-α.

Pertuzumab inhibits HRG-α-dependent cell growth of the 11_18 and Ma-24 cells. Pertuzumab inhibited cell growth stimulated by HRG-α (IC_{50} = 0.12 μg/mL) but not stimulated by EGF, TGF-α, and HB-EGF in the 11_18 cells (IC_{50} > 100 μg/mL; Fig. 2). Pertuzumab also inhibited HRG-α dependent cell growth in the Ma-24 cells (IC_{50} = 39.8 μg/mL). Isotype control human IgG1 had no effect on ligand-dependent growth in the 11_18 and Ma-24 cells (data not shown). The growth of the other cells was not affected by exposure to pertuzumab (data not shown). This finding suggests that pertuzumab selectively inhibits HRG-α-dependent cell growth.

Ligand-stimulated phosphorylation of HER receptors. The expression levels of the HER receptors in the pertuzumab-sensitive (11_18 and Ma-24 cells) and pertuzumab-resistant cell (PC-9 cells) lines were determined using western blotting (Fig. 3a). Comparison of the protein expression levels of EGFR revealed high to moderate expression in the PC-9 and Ma-24 cells. EGFR was also detected in the 11_18 cells, although the expression in this

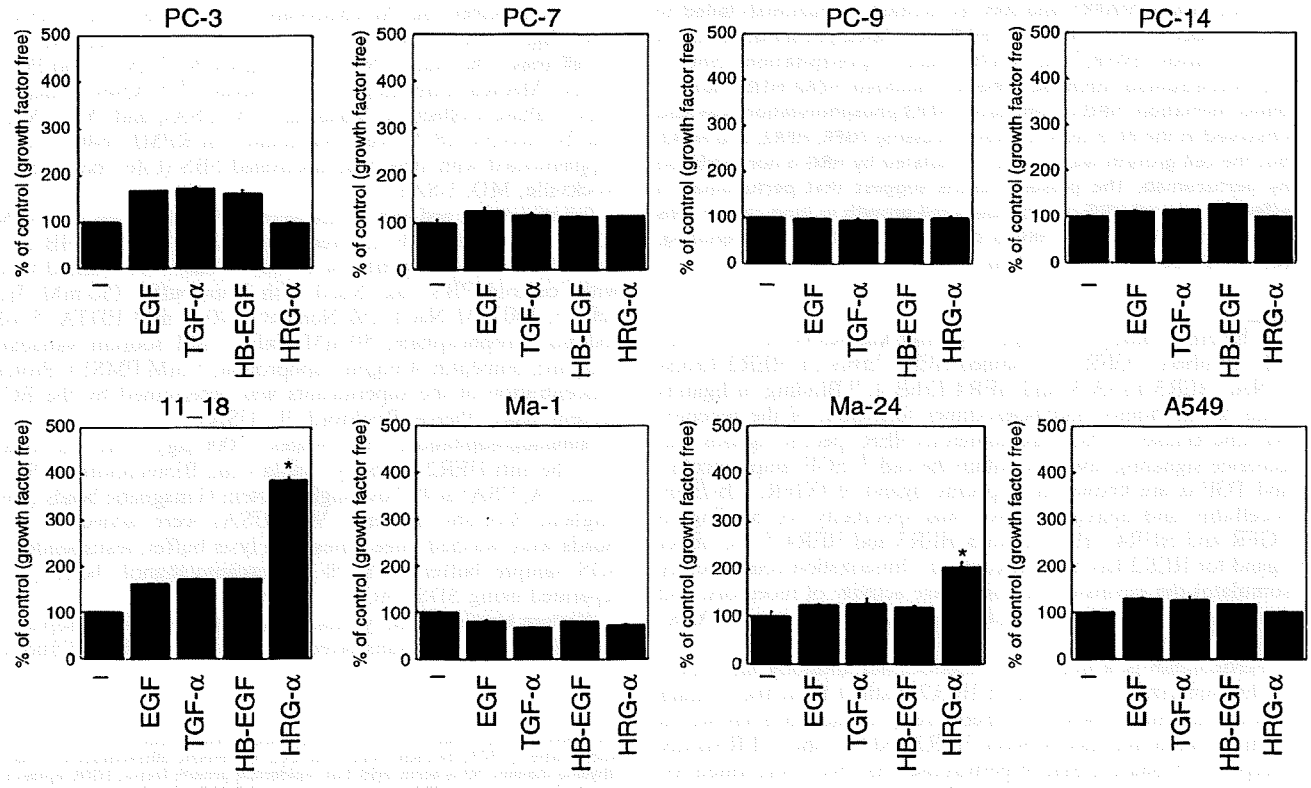

Fig. 1. Ligand-dependent cell growth in the lung cancer cells. Non-small cell lung cancer cells were stimulated with or without 100 ng/mL of epidermal growth factor (EGF), transforming growth factor (TGF)-α, heparin-binding epidermal growth factor (HB-EGF), and heregulin (HRG)-α. After incubation for 72 h, cell growth was determined using the MTS assay. The growth of cells was presented as the percentage of absorbance compared with ligand-untreated cells. Error bars represent SE. *Significant difference ($P < 0.01$; t-test) compared to the ligand-non-stimulated cells. Data shown are representative of at least three independent experiments with similar results.

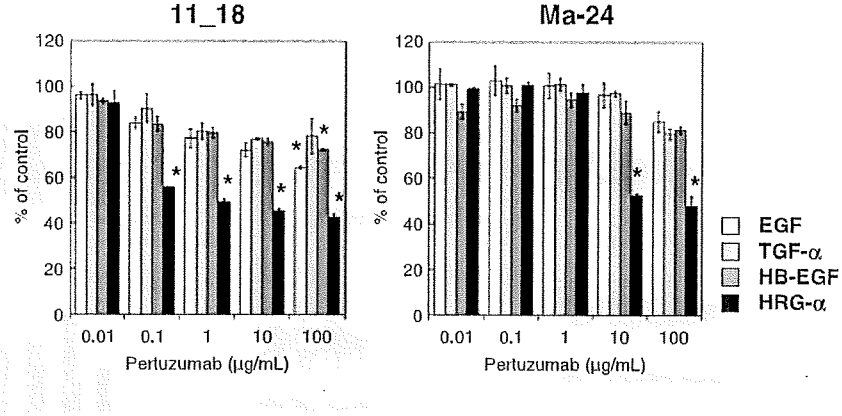

Fig. 2. Growth inhibitory effect of pertuzumab in the lung cancer cells. The lung cells were exposed to pertuzumab (0.01–100 μg/mL) for 72 h in serum free medium with or without 100 ng/mL of epidermal growth factor (EGF), transforming growth factor (TGF)-α, heparin-binding epidermal growth factor (HB-EGF), or heregulin (HRG)-α. The viability was determined using the MTS assay. Result are presented as the percentage of absorbance compared with pertuzumab-untreated cells. Error bars represent SE. *Significant difference ($P < 0.01$; *t*-test) compared to pertuzumab-untreated cells. Data shown are representative of at least three independent experiments with similar results.

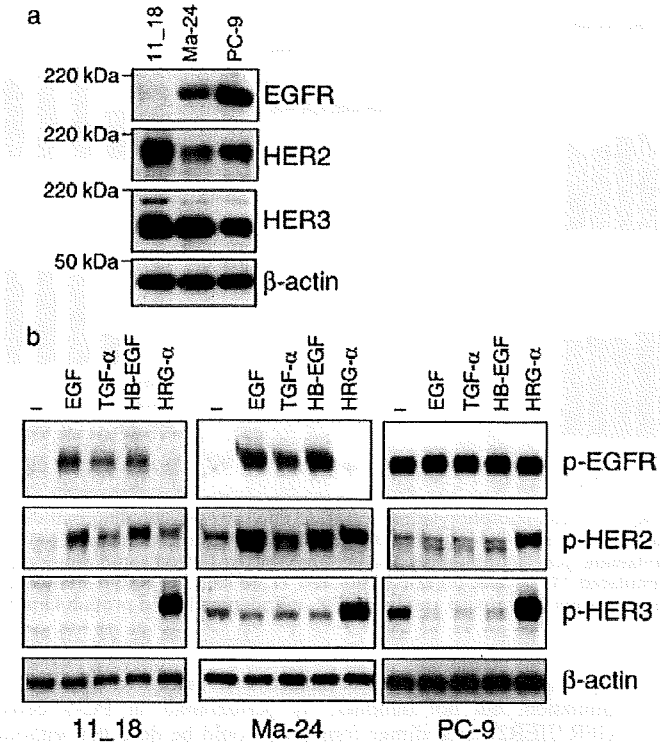

Fig. 3. Expression and phosphorylation of HER receptors in non-small cell lung cancer cells. (a) Expression of epidermal growth factor receptor (EGFR), HER2, and HER3 was detected using western blot analysis. Each lane contained 20 μg protein. β-Actin was used as a loading control. (b) The cells were stimulated with or without 100 ng/mL of epidermal growth factor (EGF), transforming growth factor (TGF)-α, heparin-binding epidermal growth factor (HB-EGF), and heregulin (HRG)-α for 10 min. Phosphorylation of EGFR and HER3 was detected using western blot analysis. Phosphorylation of HER2 was detected using immunoprecipitation followed by western blotting. β-Actin was used as a loading control. Data shown are representative of at least two independent experiments with similar results.

cell line was weak. The expression levels of HER2 were higher in the PC-9 and 11_18 cells than in the Ma-24 cells, which only expressed moderate levels of this receptor. All three cell lines showed strong expression of HER3. HER4 could not be detected in any of the three cell lines (data not shown). In contrast, these lung cancer cell lines expressed different types of EGFR mutations; the PC-9 cells had a 15-base deletion mutant (delE746-A750, exon 19), the 11_18 cells had a L858R point mutation (exon 21) of EGFR, and the Ma-24 cells had a E709G point mutation (exon 18) of EGFR. No mutations were detected in exons 19–21 of HER2 (data not shown).

Next, the ligand-stimulated phosphorylation of the HER receptors in the lung cancer cells after serum starvation was examined (Fig. 3b). While the ligands for EGFR (EGF, TGF-α, and HB-EGF) phosphorylated cellular EGFR in the 11_18 and Ma-24 cells, the EGFR in the PC-9 cells was hyperphosphorylated even under the non-stimulated condition, because PC-9 cells express an active mutant of EGFR. These results suggest that the EGF/TGF-α or HB-EGF–EGFR signals are active in lung cancer cells. The ligands for HER3 (HRG-α) specifically phosphorylated HER3 in the 11_18, Ma-24, and PC-9 cells. Phosphorylation of HER2 was analyzed by immunoprecipitation using an anti-HER2 antibody followed by western blotting for phosphotyrosine. The ligands for EGFR and HER3 phosphorylated HER2 in the 11_18 and Ma-24 cells, whereas only HRG-α but not the other ligands specifically phosphorylated HER2 in the PC-9 cells. These findings also suggest that the HRG-α–HER3 signal is active in lung cancer cells.

Pertuzumab blocks HRG-α but not EGF-stimulated signals. An inhibitory effect of pertuzumab on HRG-α-dependent cell growth in the 11_18 cells was demonstrated. To examine the effect of pertuzumab on signal transduction of both EGFR and HER3 in this cell line, the 11_18 cells were exposed to pertuzumab (0.2–200 μg/mL for 6 h) (Fig. 4a,b). HRG-α-stimulated phosphorylation of HER3 was dose-dependently inhibited by exposure to pertuzumab in the 11_18 cells, whereas EGFR phosphorylation was not stimulated by HRG-α stimulation (data not shown). MAPK and Akt were phosphorylated by HRG-α stimulation and these were inhibited by pertuzumab dose-dependently in the 11_18 cells. In contrast, EGF-stimulated phosphorylation of EGFR and MAPK was not inhibited by pertuzumab in the 11_18 cells. Phosphorylation of Akt was not detected by addition of EGF in the 11_18 cells. EGF did not phosphorylate HER3 and pertuzumab did not affect it (data not shown). Taken together, these results showed that pertuzumab inhibited HRG-α-stimulated phosphorylation of HER3, MAPK, and Akt, but not EGF-stimulated EGFR phosphorylation signaling.

HER3 is phosphorylated in response to HRG-α in the PC-9 cells as observed in the 11_18 cells, but the growth of the PC-9 cells was not increased by HRG-α (Figs 1,3b). To clarify the phosphorylation-inhibitory potential of pertuzumab, the effect of pertuzumab on signal transduction of the PC-9 cells was examined (Fig. 4c). When the PC-9 cells were stimulated by the addition of HRG-α, HER3 was phosphorylated in the PC-9 cells, but phosphorylation of HER3 was not inhibited by pertuzumab (20 and 200 μg/mL for 6 h). EGFR expressed in the PC-9 cells is constitutively active and pertuzumab failed to affect

doi: 10.1111/j.1349-7006.2007.00553.x